SEMMELWEIS EGYETEM DOKTORI ISKOLA

Ph.D. értekezések

3297.

PÁL DOMONKOS

A gyógyszerészeti tudományok korszerű kutatási irányai című program

Programvezető: Dr. Antal István, egyetemi tanár Témavezető: Dr. Turiák Lilla, tudományos főmunkatárs

MASS SPECTROMETRY-BASED ANALYSIS OF CHONDROITIN SULFATE AND HEPARAN SULFATE GLYCOSAMINOGLYCANS IN LUNG CANCER TISSUE SAMPLES USING OPTIMIZED SAMPLE PREPARATION CONDITIONS

PhD thesis

Domonkos Pál

Semmelweis University Doctoral School
Pharmaceutical Sciences and Health Technologies Division





Supervisor: Lilla Turiák, Ph.D.

Official reviewers: Borbála Dalmadi-Kiss, Ph.D.

Anikó Takátsy, Ph.D.

Head of the Complex Examination Committee:

Romána Zelkó, D.Sc.

Members of the Complex Examination Committee:

Krisztina Ludányi, Ph.D. Gitta Schlosser, Ph.D.

Table of Contents

List of	f Abbreviations	. 4
1.	Introduction	. 7
1.1.	Proteoglycans and Glycosaminoglycans	7
1.1.1.	Biosynthesis of CS/DS and HS glycosaminoglycans	. 8
1.1.2.	Role of GAGs and PGs in cancer	. 9
1.1.3.	Analytical approaches to investigate glycosaminoglycans	12
1.2.	Stability and recovery of glycosaminoglycans	15
1.3.	Lung cancer	16
1.3.1.	Subtypes of lung cancer	17
1.3.2.	Different genetic alterations of lung cancer	17
2.	Objectives	19
3.	Methods	20
3.1.	List of materials used	20
3.2.	Stability and recovery study of heparan sulfate disaccharides	20
3.2.1.	Effect of solvent type on evaporation	22
3.2.2.	Effect of freezing	23
3.2.3.	Effect of storage	23
3.2.4.	HPLC-MS analysis of HS disaccharides in the recovery and stability study	24
3.2.5.	Data analysis of the HS disaccharide stability study	25
3.3.	Analysis of lung tumor sections with different cancer subtypes	25
3.3.1.	Preparation of lung tissue sections for enzymatic digestion	26
3.3.2.	Enzymatic digestion of CS/DS GAG chains on tissue surface	27
3.3.3.	Enzymatic digestion of HS GAG chains on tissue surface	28
3.3.4.	GAG disaccharide purification with combined extraction method (cotton wool and graphite solid-phase extraction)	
3.3.5.	HPLC-MS analysis of CS/DS and HS GAG disaccharides	29
3.3.6.	Data evaluation and interpretation of lung tumor sections with different cancer subtypes	
3.4.	Analysis of lung adenocarcinoma sections with different genetic alterations	31
3.4.1.	Preparation of lung tissue sections for enzymatic digestion	31
3.4.2.	Enzymatic digestion of CS/DS GAG chains	31

3.4.3.	GAG disaccharide purification with combined extraction method (cotton woo and graphite solid-phase extraction)	
3.4.4.	HPLC-MS analysis of CS/DS GAG disaccharides	32
	Data evaluation	
4.	Results	34
4.1.	Stability studies of HS disaccharides	34
4.1.1.	Effect of solvent type on evaporation	35
4.1.2.	Effect of freezing	35
4.1.3.	Effect of storage	36
4.2.	Analysis of lung tumor sections with different cancer subtypes	46
4.2.1.	CS/DS and HS quantity and sulfation characteristics between all tumor and all tumor adjacent normal samples	
4.2.2.	CS/DS and HS content and sulfation characteristics between tumor and corresponding tumor adjacent normal samples	50
4.2.3.	CS/DS and HS sulfation between lung tumor phenotypes	52
4.3.	Analysis of lung adenocarcinoma sections with different genetic alterations	53
4.3.1.	CS/DS sulfation characteristics between the different genetic alterations	54
5.	Discussion	57
5.1.	Stability studies of heparan sulfate	57
5.2.	Analysis of lung tumor sections with different cancer subtypes	58
5.3.	Analysis of lung tumor sections with different genetic alterations	62
6.	Conclusions	65
6.1.	Stability studies of heparan sulfate	65
6.2.	Analysis of lung tumor sections with different cancer subtypes	65
6.3.	Analysis of lung adenocarcinoma sections with different genetic alterations	65
7.	Summary	66
8.	References	67
9.	Bibliography of the candidate's publications	82
9.1.	Publications Related to the Dissertation	82
9.2.	Publications Unrelated to the Dissertation	82
10.	Acknowledgements	84

List of Abbreviations

AC adenocarcinoma

ACN acetonitrile

ALK anaplastic lymphoma kinase

AMBIC ammonium bicarbonate

AUC area under the curve

CHPF chondroitin polymerizing factor7

CHSY1 chondroitin sulfate synthase 1

CRC colorectal cancers

CS chondroitin sulfate

CSGALNACT1 chondroitin sulfate *N*-acetylgalactosaminyltransferase 1

CSPG chondroitin sulfate proteoglycan

D4ST dermatan 4-sulfotransferase

D4ST1 dermatan 4-*O*-sulfotransferase 1

Da dalton

dp12 dodecasaccharide

DS dermatan sulfate

DSE1 dermatan sulfate epimerase 1

DSE2 dermatan sulfate epimerase 2

ECM extracellular matrix

EGFR epidermal growth factor receptor

EIC extracted ion chromatograms

ER endoplasmic reticulum

ESI electrospray ionization

EXT1 exostosin glycosyltransferase-1

EXT2 exostosin glycosyltransferase-2

FFPE formalin-fixed, paraffin-embedded

GAG glycosaminoglycan

GalNAc *N*-acetylgalactosamine

GlcA glucoronic acid

GlcNAc N-acetylglucosamine

HILIC-WAX hydrophilic interaction liquid chromatography combined with

weak anion exchange

HPLC high-performance liquid chromatography

HS heparan sulfate

IdoA iduronic acid

KRAS Kirsten rat sarcoma viral oncogene homolog

LC lung cancer

LCC large cell carcinoma

MALDI matrix assisted laser desorption ionization

MeOH methanol

MS mass spectrometry

NB-1 human neuroblastoma cell line

NDST1-4 *N*-deacetylase/*N*-sulfotransferases

NMR nuclear magnetic resonance

NSCLC non-small cell lung cancer

ofCS oncofetal chondroitin sulfate

PG proteoglycan

PTM post-translational modification

Q-TOF quadruple time of flight

RTK receptor tyrosine kinase

SCLC small cell lung cancer

SD standard deviation

SPE solid-phase extraction

SpeedVac heated vacuum concentrator

SqCC squamous cell carcinoma

SRGN serglycin

TFA trifluoroacetic acid

TRIS-HCl tris(hydroxymethyl)aminomethane hydrochloride

UDP uridine diphosphate

UDP- GalNAc uridine diphosphate *N*-acetylgalactosamine

UDP-GlcA uridine diphosphate glucoronic acid

UPLC ultrahigh performance liquid chromatography

WT wild-type

1. Introduction

1.1. Proteoglycans and Glycosaminoglycans

Proteins are complex macromolecules that play a vital role in the functioning of living organisms. Their activity and roles can be significantly influenced by post-translational modifications (PTMs), mainly located on the side chains of the amino acids (1,2). Glycosylation is a widely studied PTM, where sugar units are covalently attached to proteins, most often through an oxygen or nitrogen atom (*O*- and *N*-glycans) (3,4). The term glycoprotein is used when a carbohydrate is linked to a protein (5).

Proteoglycans (PGs) are a special class of glycoproteins characterized by a core protein and one or more glycosaminoglycan (GAG) chains covalently attached predominantly to serine amino acids through a tetrasaccharide linker (**Figure 1**). PGs are principally located in the extracellular matrix (ECM) and in the plasma membrane, thus playing important roles in the stabilization of the extracellular matrix and signaling processes (3).

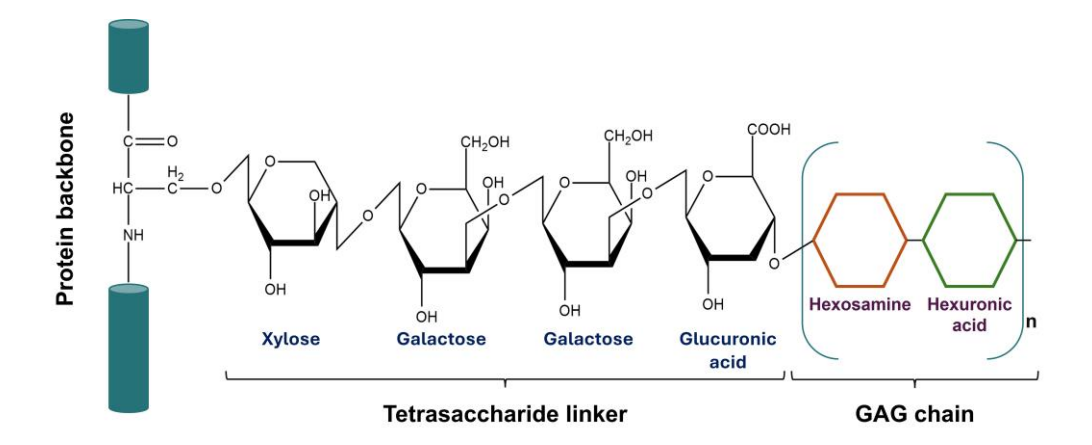


Figure 1. General structure of heparan sulfate and chondroitin/dermatan sulfate proteoglycans, showing the three building units: the core protein, the tetrasaccharide linker and the GAG chain.

GAGs are linear polysaccharides consisting of repeating amino sugar and uronic acid or galactose disaccharide building blocks. GAGs influence the functions of cells through their interactions with growth factors and cytokines (6). Chain size and structural diversity including sulfation characteristics of GAGs have a significant impact on the functions of GAG-binding proteins (7,8). The sulfation pattern of GAG chains is formed by sulfotransferase enzymes (9). Chondroitin sulfate (CS) and heparan sulfate (HS) are among the most widely studied GAG classes, due to their abundance in tissues, their well-characterized biosynthetic pathways and critical roles in cell signaling, adhesion and development. CS chains consist of *N*-acetylgalactosamine (GalNAc) and glucoronic acid

(GlcA), while HS chains are composed of *N*-acetylglucosamine (GlcNAc) and glucuronic/iduronic acid (IdoA) units. The structural diversity of CS and HS arises from various possible sulfation sites in their disaccharide building units. CS and DS GAG classes are often considered together (CS/DS), because they share structural similarities with each other. The difference is that DS contains IdoA instead of GlcA. The ratio of CS and DS plays a crucial role in the development of various tissues (10).

1.1.1. Biosynthesis of CS/DS and HS glycosaminoglycans

Since GAGs have many crucial biological functions, knowledge of their biosynthesis is essential to understand their precise role in various diseases (11).

Synthesis of CS/DS chains occurs simultaneously following the production and attachment of the tetrasaccharide linker to the protein. The CS-synthesizing enzymes use cytosolic-derived uridine diphosphate -GlcA (UDP-GlcA) and UDP-GalNAc (12). The transport of UDP sugars from the cytosol to the Golgi apparatus and endoplasmic reticulum (ER), where GAG synthesis takes place, is a crucial step (13). For DS synthesis, some of the GlcA residues left over from CS synthesis are epimerized to IdoA by chondroitin GlcA-C5 epimerase/DS epimerases (DSE1 and 2). Therefore, the biosynthetic process of CS/DS is catalyzed by glycosyltransferases, epimerases and sulfotransferases and regulated by UDP-glucose dehydrogenase (14). CS polymerization requires the activity of glucuronyltransferase II and N-acetylgalactosaminyltransferase II (15). During this elongation phase, the size of CS and DS chains is determined, ranging from 40 to over 100 disaccharide units, with molecular weight between 5-50 kDa. The position of sulfate groups has an impact on the interactions of CS chains. Dermatan 4sulfotransferase (D4ST) leads to the sulfation of the C4 position of GalNAc residues, causing the formation of IdoA-GalNAc4S-rich cluster in DS chains. DSE-1, in contrast with DSE-2, can interact with D4ST to facilitate the synthesis of longer IdoA-containing chains (16). Sulfate group position and the epimerization of GlcA residues may influence the structure, conformation and dynamics of CS4, CS6, and DS, as evidenced by molecular dynamics analyses showing distinct variations among these subtypes (17). The 4-O-sulfation of GlcA residues by dermatan 4-O-sulfotransferase 1 (D4ST1) is essential for stabilizing epimerization (16,18).

The biosynthesis of HS also occurs in the Golgi apparatus and involves the following three main phases: synthesis of the tetrasaccharide linker, elongation of the proheparan

chain, and modifications leading to mature sulfated HS chains (19,20). At least 26 enzymes are involved in this process (19,20). The elongation begins with the addition of *N*-acetylglucosamine to the tetrasaccharide linker. The GlcNAc residues undergo several modifications such as *N*-deacetylation and *N*-sulfation by *N*-deacetylase/*N*-sulfotransferases (NDST1-4). Further modifications involve C5 epimerization of GlcA to IdoA next to GlcNS. The sulfation of HS chains is catalyzed by HS 6-*O*- and 3-*O*-sulfotransferases at C6 of GlcNAc or GlcNS and C3 of GlcN. The length of HS chains often range from 50 to over 150 disaccharide with an average molecular weight of 30 kDa. The enzymes, which are involved in the biosynthesis of HS chains, interact and form a GAGosome complex regulating the enzymatic activities (20,21).

Deviations in the biosynthesis of CS and HS GAGs are implicated in a number of genetic and acquired diseases. Mutations in enzymes such as chondroitin sulfate *N*-acetylgalactosaminyltransferase 1 (CSGALNACT1) and chondroitin sulfate synthase 1 (CHSY1), which are involved in CS biosynthesis, can lead to severe congenital skeletal abnormalities including Desbuquois dysplasia and spondyloepimetaphyseal dysplasia. Furthermore, mutations in glycosyltransferases encoding genes like exostosin glycosyltransferase-1or-2 (EXT1 or EXT2), are required for the elongation of HS chains, results in hereditary multiplex exostosis, which is characterized by abnormal bone growths (12,13). Progressive neurological, skeletal, and cardiovascular symptoms arise from impaired degradation of HS and/or CS, as seen in mucopolysaccharidoses types I, II, and VI, associated with specific enzyme deficiencies. (13,14). In addition, connection between the dysregulated biosynthesis of HS and neurodevelopmental conditions such as autism spectrum disorder and schizophrenia, as well as neurodegenerative diseases such as Alzheimer's disease, where abnormal sulfate formation patterns may influence protein aggregation and synaptic stability, have been reported (15, 16).

1.1.2. Role of GAGs and PGs in cancer

PGs are key players in maintaining the structure of the extracellular matrix and regulating signal transduction processes. As a result, any changes in their glycosylation can significantly affect their function and alter various signaling pathways in the tumor microenvironment (22). The literature clearly shows that altered protein glycosylation is a common feature of cancer. GAGs and PGs are deeply involved in cancer progression, primarily through their role in modulating expression and activity of enzymes, which are

critical in their metabolism (22–26). One of their key functions in the tumor microenvironment is the regulation of cancer cell proliferation by acting as coreceptors for growth factor receptors, forming complexes that amplify signaling pathways (27). These interactions enable GAGs to influence vital processes including tumor growth, angiogenesis, invasion, and metastasis (28). Furthermore, GAGs are not only tumor promoters, they also have inhibitory roles. For example, heparanase enzyme contributes to tumor progression by releasing growth factors bound to heparan sulfate PGs, thereby enhancing growth factor availability and downstream activation (22,27). Differences in the total quantity and sulfation characteristics of GAG chains have been observed between healthy and cancerous tissues. Such variations in GAG expression have been reported in various cancer types, including lung cancer. Additionally, higher levels of branched *N*-glycans and increased proportion of *O*-glycans (29) have been found in lung cancer.

Changes in the expression of GAGs, PGs, and enzymes (glycosyltransferases, epimerases, sulfotransferases) have a significant regulating role throughout all stages of cancer development and also carry important prognostic value (24). For instance, mutations in genes EXT1, EXT2, which encode essential enzymes for HS chain synthesis, are associated with hereditary multiple exostoses and development of malignant chondrosarcomas (30). In a model of colon epithelial cell transformation, HS undergoes significant structural changes, including a 33% reduction in 2-*O*-sulfation and a 20% decrease in *N*-sulfation during the transition from adenoma-like to carcinoma-like states (31). These changes can significantly influence how HS proteoglycans (HSPGs) interact with ligands, ultimately affecting their biological activity.

The increased level of CS/DS GAGs have been associated with neoplastic tissues, that have suffered abnormal and uncontrolled cell growth, while a decrease in the quantity of HS is a typically observed phenomenon. (32). Expression of sulphated GAGs and PGs in cells can be altered during tumor progression (33). Modification of CS and HS GAGs on PGs can affect their function (34). In addition, it has been observed that PG degradation fragments may retain biological activity (35). Reduced levels of HS are consistent with its known role in regulating cell-cell interactions and cell cycle inhibition (36). On the other hand, the observed increase in CS/DS may contribute to enhanced cell proliferation.

This is supported by the fact, that CS synthesis leads to cytokinesis failure and early embryonic death, highlighting the role of CS in cell division (37).

Colorectal cancers (CRCs) are typically categorized as right- and left-sided tumors, which differ not only in their clinical presentation and surgical approaches but also in their underlying molecular characteristics, including biomarker profiles (38). A key molecular alteration during CRC progression involves HSPGs. These changes affect both the core protein and their GAG chains, playing a significant role in malignant transformation (32). Alterations in HSPGs are not unique to CRC, they have been observed in wide range of cancers including brain, breast, lung, skin, pancreas, colon, ovarian, head and neck cancers. These changes are associated with tumor behaviour, influencing cell signaling, adhesion, migration, angiogenesis, and survival (39).

The expression patterns of HSPGs are shaped by the cell-type-specific expression of

various biosynthetic enzyme isoforms (40). In CRCs, gene expression analyses related to HSPG biosynthesis show that non-metastatic tumors exhibit altered expression in 40% of relevant genes, especially those involved in CS chain polymerization and modification. However, metastatic tumors show changes in fewer than 20% of these genes, mainly involving enzymes responsible for structural modifications. All the gene alterations found in metastatic CRCs also appeared in non-metastatic cases, with the exception of syndecan-1 and chondroitin polymerizing factor (CHPF). HS chains were less affected in metastatic tumors compared to non-metastatic ones. Furthermore, meanwhile cell surface PGs varied in expression depending on metastatic status, PGs found in the extracellular matrix or intracellularly exhibited consistent expression regardless of metastasis (38). Decorin, a small leucine-rich PG, has emerged as a promising candidate for cancer therapy due to its ability to modulate key oncogenic signaling pathways. In preclinical studies using a mammary carcinoma model, treatment with decorin led to a 70% reduction in tumor growth and effectively prevented metastasis, primarily by modulating epidermal growth factor receptor (EGFR) signaling and promoting receptor downregulation (44, 59). Delivering decorin through adenovirus vectors has shown similar anti-tumor effects (42). In xenograft models, decorin not only suppressed tumor growth and angiogenesis, but also increased levels levels of the cell cycle regulator p21WAF1, a potent cyclindependent kinase inhibitor that regulates cell cycle progression (60, 61). Additionally,

decorin expression has been linked to improved survival in a rat glioma model (44).

Despite these promising results, bringing decorin into clinical use remains difficult due to the molecular variability of its GAG chains which poses a challenge for consistent and scalable production (44).

There has been growing interest in understanding how PGs are expressed in normal prostate tissue, particularly as a baseline for studying their alterations in prostate cancer, given their key roles in regulating tumor growth and progression (45). Previous research has identified the presence of several PGs in prostate cancer, including versican (46), decorin (47), lumican (48), and syndecan-1 (49,50). Among these PGs, versican is outstanding as the most consistently expressed extracellular proteoglycan in prostate tumors. Notably, the mRNA levels of versican were similar in both cancerous and noncancerous prostate tissue, suggesting that its build-up in tumors might result from factors like altered protein degradation or post-transcriptional regulation, rather than increased gene transcription. In contrast, decorin was typically found in lower expression levels in tumor tissues, although the extent of reduction varied between samples, possibly accounting for inconsistencies reported in different studies (45). Lumican, meanwhile, showed consistent expression across both normal and cancerous prostate tissues (45). In normal tissue, glypican-1 was primarily found in ephitelial cells, but its expression dropped in cancerous epithelial cells, while an increase was found in the surrounding tumor stroma (51). In the case of syndecan-1, a similar trend was observed, with reduced expression in cancer epithelial cells and elevated levels in the stroma. The loss of syndecan-1 in epithelial cells has been associated with higher tumor grade in head and neck squamous cell carcinomas and has been linked to worse outcomes in gastric cancer (52).

These findings highlight the complex roles of GAGs and PGs in cancer biology (53). Alterations in their expression and structure in different types of tumors points to their potential both as biomarkers and therapeutic targets.

1.1.3. Analytical approaches to investigate glycosaminoglycans

The analysis of GAGs is a complex task due to their size and structural diversity. Intact GAG chains can be analyzed by means of nuclear magnetic resonance (NMR) spectroscopy, size-exclusion chromatography, high-performance liquid chromatography (HPLC), and high-resolution tandem mass spectrometry (MS) (54–56). Antibody-based techniques are powerful tools to investigate specific GAG types, sulfation motifs or

distribution in cells and tissues (57). Sulfation patterns and the quantity of different GAG saccharide species can also be carried out at the oligosaccharide or disaccharide levels, which requires the breakdown of the GAG chains prior to analysis. This depolymerization can be achieved by two methods: enzymatic and chemical cleavage. The enzymatic digestion is performed by bacterial enzymes, while chemical cleavage is carried out with nitric acid. During enzymatic digestion, the products lose their stereochemical integrity, whereas it is preserved in chemical breakdown. (56). The structure and nomenclature of the most commonly occurring disaccharides produced by the enzymatic digestion of CS and HS GAG chains are shown in **Table 1** and **Table 2**, respectively. The simplified nomenclature developed by Lawrence et al., the Lawrence code, is widely used to provide a simpler and clearer name for the repeating disaccharide units of GAG chains (**Table 1** and **Table 2**) (58).

Table 1. The molecular structure, the traditional name, the Lawrence code, the analyzed ions and m/z values of the CS/DS disaccharides in negative mode. The D0a4 and D0a6 disaccharides are positional isomers and their differentiation was made via MS/MS transition.

Disaccharide structure	Traditional name	Lawrence code	Detected ion	m/z	MS/MS transition
OH OH OH OH NHAC	ΔHexA-GalNAc	D0a0	[M-H] ⁻	378.10	
OH OH NHAC	ΔHexA-GalNAc4S	D0a4	[M-H] ⁻ [M-2H+Na] ⁻ [M-2H+K] ⁻ [M-2H] ²⁻	458.10	300.10
OH OH ON OH NHAC	ΔHexA-GalNAc6S	D0a6	[M-H] ⁻ [M-2H+Na] ⁻ [M-2H+K] ⁻ [M-2H] ²⁻	458.10	282.10
OH OH NHAC	ΔHexA- GalNAc4S6S	D0a10	[M-H] ⁻ [M-2H+Na] ⁻ [M-2H+K] ⁻ [M-2H] ²⁻	538.05 560.05 576.00 268.50	

Table 2. The molecular structure, the traditional name, the Lawrence code, the analyzed ions and m/z values of the HS disaccharides. In the first project only the D0A6 and D0S6 isomers were investigated. In the second project D2A0/D0A6 and D2S0/D0S6 isomers were not differentiated.

Disaccharide structure	Traditional name	Lawrence code	Detected ion	m/z
OH HO NHAC OH	ΔHexA-GlcNAc	D0A0	[M-H] ⁻	378.10
OH HO NHAC OH	ΔHexA2S-GlcNAc	D2A0	[M-H] ⁻	458.10
OH HO3SO OH NHAC OH	ΔHexA-GlcNAc6S	D0A6	[M-H] ⁻	458.10
OH HO NHSO,H	ΔHexA-GlcNS	D0S0	[M-H] ⁻ [M-2H+Na] ⁻	416.10 438.10
OH HO3SO OH NHAC OH	ΔHexA2S- GlcNAc6S	D2A6	[M-H] ⁻ [M-2H+Na] ⁻ [M-2H+K] ⁻ [M-H-SO ₃] ⁻ [M-2H] ²⁻	538.10 560.10 576.10 458.10 286.55
OH HO NHSO ₃ H HO NHSO ₃ H	ΔHexA2S-GlcNS	D2S0	[M-H] ⁻ [M-2H+Na] ⁻ [M-H-SO ₃] ⁻ [M-2H] ²⁻	496.10 518.10 416.10 247.55
OH HO3SO OH NHSO3H	ΔHexA-GlcNS6S	D0S6	[M-H] ⁻ [M-2H+Na] ⁻ [M-H-SO ₃] ⁻ [M-2H] ²⁻	496.10 518.10 416.10 247.55
OH HO3SO OH NHSO3H	ΔHexA2S-GlcNS6S	D2S6	[M-H] ⁻ [M-2H+Na] ⁻ [M-2H+K] ⁻ [M-H-SO ₃] ⁻ [M-2H] ²⁻ [M-3H+Na] ²⁻	576.10 598.10 614.10 496.10 287.55 298.55

After the digestion the GAG oligo- and disaccharides are generally analyzed by chromatographic or electrophoretic methods (59). These involve the use of liquid chromatography or capillary electrophoresis with MS or fluorescence detection following derivatization (60,61). The study of GAGs relies heavily on effective separation techniques, as their structural diversity, varying degrees of sulfation and their extreme polarity present significant analytical challenges. GAG disaccharides have been extensively studied in the literature using various separation techniques (56). Among these approaches, reversed-phase chromatography with derivatization or ion-pair formation, hydrophilic interaction chromatography (HILIC), and hydrophilic interaction

chromatography combined with weak anion exchange chromatography (HILIC-WAX) have been identified as the most reliable methods (62–64).

MS detection techniques are among the most sensitive approaches for GAG analysis. Both electrospray ionization (ESI) and matrix-assisted laser desorption ionization (MALDI) can be used depending on the aim of the study (65,66). These ion sources are classified as soft ionization techniques, which is essential to prevent the undesired loss of sulfate groups, which are highly susceptible to fragmentation and contribute to structural instability (67). Furthermore, the presence of sulfate groups with acidic character on GAGs requires the use of a negative ionization mode in the case of native analysis. Our research group has previously developed HPLC-MS methods for sensitive CS and HS disaccharide analysis using HILIC-WAX-based capillary chromatography (62,68,69). Introducing the use of salt gradients allowed for shorter analysis time (15 min) and more reliable quantification of small amounts of HS and CS disaccharides (10-20 fmol) extracted from tissue surfaces (68–70).

The bioinformatic evaluation of GAGs is a complex task that must fulfill several criteria (71). The detailed analysis of disaccharides is conducted by examining general patterns, providing a straightforward and sufficiently reliable approach for effective evaluation.

1.2. Stability and recovery of glycosaminoglycans

The analysis of GAG samples of biological origin requires several sample preparation steps. The general workflow involves enzymatic digestion or chemical cleavage of the large polysaccharide chains into oligo- or disaccharides to facilitate their analysis by HPLC-MS. This is followed by solid-phase extraction (SPE) purification, evaporation, freezing, and thawing. These steps may include intermediate steps like sample transfer and storage, which can also lead to significant sample loss. For HS disaccharides the solvent evaporation, freezing and storage are the most critical factors affecting stability and recovery. These factors are heavily influenced by solvent type, the material of the storage vessels, temperature, and pH. In addition, the results of the analytical measurements can be further hindered by adsorption on surfaces or chemical degradation. GAG disaccharides are most frequently desalted using SPE, which requires solvent change during and after the cleaning process (72). The solvent change steps involve evaporation, which creates the necessary conditions for the subsequent steps of the workflow; however, they have a significant impact on recovery.

Several parameters influencing the stability and recovery of CS disaccharides has been previously investigated (73). The highest recovery values were obtained when CS disaccharides were evaporated from low volumes of aqueous solutions using a heated vacuum centrifuge. The degradation of CS disaccharides can occur during autosampler storage, but the sample loss can be reduced if the storage is performed in acetonitrile (ACN) containing solvents instead of methanol (MeOH) containing ones (73). Under neutral conditions at elevated temperatures, the degradation of CS chains occurs, resulting in smaller monomer (glucuronic/iduronic acid or GalNAc) and desulfated fragments (74). As HS disaccharides may contain more sulfate groups than CS disaccharides, their stability may be more significantly affected by the impact of storage and sample preparation; however, there is a lack of literature on the stability and recovery of HS disaccharides. The degradation of heparin, which has a very similar structure to HS GAGs, has been studied previously. Heparin is performed by mast cells and has a higher sulfate density and contains more iduronic acid residues compared to HS. Kozlowski et al. studied the acid hydrolysis of heparin at 40, 60 and 80 °C. Their results indicated that heparin remained resistant to glycosidic cleavage at pH 1-6 between 40 and 60 °C. However, after 24 h at pH 1 at 80 °C, the occurrence of glycosidic cleavage has been identified (75). Under basic conditions (pH 9 or above), over 50 °C, side reactions happen on the heparin backbone, such as 2-O-desulfation (76). Janik et al. examined the degradation pathways of heparin by analyzing sodium heparin under acidic and basic conditions at 30 and 60 °C. Heparin exhibited a remarkable stability in the first 500 hours, but between 1000 and 2000 h rapid degradation occurred. The identified decomposition under these conditions involves the internal hydrolysis of glycosidic linkages and loss of N-sulfate groups in particular (77). A significant proportion of the errors encountered in the analytical workflow of GAGs arise from the sample preparation process; therefore, it is crucial to study the stability and recovery of the components of interest under the parameters used during the sample preparation process. The choice of optimal conditions can reduce the number of anomalies that occur during measurements, which is likely to allow significantly more accurate analysis of biological samples.

1.3. Lung cancer

Lung cancer (LC) is the most frequently diagnosed cancer type considering both men and women and holds the highest mortality rate globally (2022), since the majority of cases

are detected at an advance stage (78). Moreover, the treatment options are limited and metastasis occurs frequently to other organs (79,80).

1.3.1. Subtypes of lung cancer

Histologically LC can be categorized into two primary groups: small cell lung cancer (SCLC) and non-small cell lung cancer (NSCLC). NSCLC constitutes approximately 85%, while SCLC for 15% of all LC cases (81). NSCLC is a heterogeneous group and can be further categorized into adenocarcinoma (AC), squamous cell carcinoma (SqCC) and large cell carcinoma (LCC) (81–83). AC is the predominant subtype, accounting for 40% of all NSCLC cases, originates from the glandular epithelium (81–83). Treatment strategies for SCLC and NSCLC are primarily determined by tumor type and progression stage, and may involve surgery, radio-chemotherapy, targeted therapies such as antiangiogenic monoclonal antibodies or tyrosine kinase inhibitors, and immunotherapy (82,84). The increased proportion of branched N-glycans and the increased amount of Oglycans have already been reported in relation to lung cancer (4,85,86). Furthermore, differences in the total quantity and in the sulfation patterns of GAG chains have also been observed between healthy and tumor tissues (87-89). Previous studies have investigated CS and HS chains in the context of lung cancer (90-92). However, these initial studies primarily focused on comparing the total GAG content and different GAG classes between LC samples and normal tissues (90), as well as among distinct LC types (91), utilizing small sample cohorts (n = 11 and 13). HPLC-MS analysis of disaccharides from SqCC tissues and corresponding normal tissues (n = 10) has been conducted (92); however, comparative studies at the disaccharide level across different LC subtypes remain unexplored, despite the growing evidence that GAGs have crucial roles in tumor progression, metastasis, and immune evasion.

1.3.2. Different genetic alterations of lung cancer

Multiple genetic alterations in key oncogenes have been identified in lung AC, including *EGFR*, Kirsten rat sarcoma viral oncogene homolog (*KRAS*), and anaplastic lymphoma kinase (*ALK*) (93,94). These genetic alterations have been identified as oncogenic drivers of AC possessing predictive value for targeted therapies (95). Mutations in genes such as EGFR, KRAS and ALK can serve as specific molecular targets offering prognostic value (96,97). Mutations in EGFR gene occur in approximately 30-40% of NSCLC cases, with a higher frequency observed in AC, non-smokers, females (95,98–101). Exons are

segments of a gene that contain coding information for protein synthesis. The most prevalent EGFR mutations are exon 19 deletion and the L858R point mutation in exon 21, collectively accounting for approximately 85% of cases (102). Mutation in exon 19, as well as mutation in exon 18 and 21, are frequently associated with increased sensitivity to EGFR tyrosine kinase inhibitors. Conversely, exon 20 insertion mutations often correlate with reduced sensitivity to these (103). ALK rearrangements are detected in approximately 2-7% of NSCLC patients, with a higher prevalence among younger individuals and non-smokers (95, 98–100). ALK rearrangements are considered adverse indicators in patients with surgically resected AC; however, EGFR mutations are generally associated with a more favorable prognosis (100). KRAS gene mutations are detected in approximately 25% of NSCLC cases, with higher prevalence among males and a significantly greater occurrence in smokers and former smokers compared to non-(93,95,98,99). It has shown that, in primary AC both EGFR and KRAS smokers mutations are also targetable (104). The proteins encoded by the ALK and EGFR genes are both tyrosine kinase receptors, while KRAS acts as a downstream effector of EGFR. These proteins activate the RAF/MEK/MAPK and PI3K/AKT signaling pathways, driving cell growth and proliferation (105,106). These signaling pathways have become important targets for precision therapies aimed at blocking oncogenic signaling in patients with specific mutations (107–109).

2. Objectives

The dissertation is based on three interlinked research projects. The work was approved by the Medical Research Council (TUKEB), ethical permit number: IV/2567-4/2020/EKU, 22/04/2020.

The objective of the first project (110) was to optimize our sample preparation process including sample handling and storage through a comprehensive study comparing common parameters and methods for analyzing HS samples of biological origin, aiming to reduce biases arising from sample loss during sample preparation. For HS sample preparation the common workflow includes HS chain extraction, digestion into disaccharides, derivatization, purification, and analysis. This multi-step process involves several intermediate sample handling steps that have a great impact on the results. Therefore, we have systematically examined the type of buffer used for digestion, injection conditions, solvent evaporation and freezing cycles for storage. An additional objective was to evaluate factors influencing sample stability and recovery to ensure more reliable and reproducible HS analysis.

The aim of the second project (111) was to investigate the compositional differences of CS/DS and HS disaccharides in different lung tumor phenotypes and adjacent normal lung tissue samples and to draw conclusions about quantitative and qualitative changes, which could be potentially used for diagnostic or therapeutic purposes. The investigation was done through tissue surface enzymatic digestion, followed by SPE purification and HPLC-MS measurements, using a custom-packed capillary column with HILIC-WAX mixed solid phase resin, and negative ionization mode detection.

In the course of the third project (112), we performed a comprehensive investigation of CS/DS disaccharide composition in lung AC tissues with ALK, EGFR and KRAS genetic alterations, and compared these profiles with triple wild-type (WT) lung AC tumors. These genetic alterations not only drive distinct oncogenic signaling pathways but may also influence the composition and remodeling of the tumor extracellular matrix, including GAGs. We aimed to uncover GAG signatures that reflect tumor biology and microenvironmental adaptations associated with specific mutations. Such insights could ultimately help in identifying novel biomarkers for patient stratification, predict responses to targeted therapies, and reveal GAG-modifying enzymes or structural motifs as potential therapeutic targets to complement existing treatments.

3. Methods

3.1. List of materials used

LC-MS-grade acetonitrile, crystalline ammonium formate, ammonium bicarbonate, chondroitinase ABC, calcium hydroxide, formic acid, trifluoroacetic acid, tris-(hydroxymethyl)-amino-methane were purchased from Merck (Darmstad, Germany). Distilled water, methanol, xylene, ethanol (abs.) and glycerol (50%) were obtained from VWR Internationals (Debrecen, Hungary). The $\Delta 4,5$ -unsaturated heparan sulfate and chondroitin sulfate disaccharide standards and heparin lyase I-II-III enzymes were purchased from Iduron Ltd. (Manchester, UK). Ammonia (25%) was purchased from Reanal (Budapest, Hungary). Pierce graphite spin column and GlycanPac AXH-1 analytical column (1.9 μ m, 2.1 \times 150 mm) were obtained from Thermo Fisher Scientific (Waltham, MA USA). Cotton wool was bought from DM-Drogerie Markt (Karlsruhe, Germany).

3.2. Stability and recovery study of heparan sulfate disaccharides

To investigate the parameters affecting stability and recovery of HS disaccharides, commercially available HS disaccharide standards were used. Our study focused on six common HS disaccharides (Table 2.), excluding their isomeric counterparts, as they are expected to behave similarly under the study conditions. For our experiments all the samples and their control samples were prepared together in one batch. The HS disaccharide stock solution concentration was 50 pmol/µL. The final concentration of the D0S6 and D2S6 disaccharides was 2500 fmol/µL, while for D0A0, D0A6, D0S0 and D2A6 disaccharides it was 500 fmol/µL. The total sampling volumes of the investigated disaccharides, the dilution volumes and the number of the investigated samples are detailed in Table 3. Due to the high number of samples, in certain cases, the sample preparation was carried out in multiple cycles, with B1-B4 representing the batch number of the sample preparation cycle. 10 µL portions of the samples were dried and stored frozen, until further handling (reconstitution, storage, etc.) which were performed based on the tested conditions outlined in the following subsections (Table 4.). For multiple batches, several control samples were prepared, ensuring that each sample was compared to its corresponding batch-specific control.

Table 3. Detailed measurement volumes and sample numbers investigated in each condition. B1–B4 indicate different preparation batches due to the high number of samples.

	Measured quantity of D0S6; D2S6 from stock (μL)	Measured quantity of D0A0, D0A6, D0S0, D2A6 from stock (μL)	Measured quantity of water used for dilution (μL)	Number of 10 μL aliquots
Effect of evaporation study	21	4.2	291.2	30
Effect of freezing	18	3.6	300	25
Effect of storage				
Temperature	21	4.2	291.2	30
рН	B1: 27 B2: 30	B1: 5.4 B2: 6.0	B1: 374.4 B2: 416.0	B1: 40 B2: 45
Enzyme buffers	18	3.6	300	25
Solvents	B1: 27 B2: 27 B3: 27 B4: 18	B1: 5.4 B2: 5.4 B3: 5.4 B4: 3.6	B1: 374.4 B2: 374.4 B3: 374.4 B4: 249.6	B1: 40 B2: 40 B3: 40 B4: 25
Vessels	21	4.2	291.2	30

For the analysis, each sample was dissolved in 10 mM ammonium formate 75:25 ACN:water (pH 4.4) (our commonly used injection solvent), the final sample volume was $12~\mu L$ of which $1~\mu L$ was injected for investigation in the case of each conditions. During the experiment five parallel and control samples were measured in each investigated conditions. Control samples were prepared in the same batch, only leaving out the respective sample preparation steps. For control sample standard HS disaccharides were dissolved in water, dried and stored frozen until analysis. The investigated conditions and parameters are summarized in **Table 4.** All the samples were stored in 0.5 mL plastic Eppendorf Safe-Lock Tubes (Eppendorf Corporate), unless otherwise is stated. For the HPLC-MS analysis the samples were stored in borosilicate 70 glass vial with glass insert (LAB-EX Kft.) and injected by autosampler.

Table 4. Summary of the investigated conditions and parameters.

Aspect of the investigation	Investigated conditions	Used parameters	
Evaporation	-	12.5 mM AMBIC Water 20 mM TRIS-HCl	
Freezing	Freezing (samples in 50 μL water) and thawing with block heater.	-20 °C (freezer) -196 °C (liquid nitrogen) 5 or 10 cycles	
Storage			
Temperature	The samples in 50 μ L water were stored under different temperatures for 48 hours.	-18 °C; 4 °C; 20 °C; 37 °C; 55 °C	
рН	The samples in 50 μL solution were stored at different pH values at 37 $^{\circ}C$.	pH=3 (1 mM hydrochloric acid) pH=7 (water) pH=11 (1 mM NaOH) 0; 6; 12; 24 hours storage	
Digestion buffer	The samples were stored in different digestion buffers (50 μ L) at 37 $^{\circ}$ C.		
Solvents	The samples were stored in different solutions (20 μ L) at 4 °C.	90:10 v/v% ACN:water 75:25 v/v% ACN:water 50:50 v/v% ACN:water 10 mM ammonium formate in 75:25 v/v% ACN:water 75:25 v/v% MeOH:water 10 mM ammonium formate in 75:25 v/v% MeOH:water 0; 6; 12; 24 hours storage	
Vessels	The samples were stored in different vessels (20 μ L) at 4 $^{\circ}$ C.	Plastic Eppendorf Safe-Lock Tube Borosilicate type 70 glass vial 10 mM ammonium formate in 75:25 v/v% ACN:water Water 24 hours storage	

3.2.1. Effect of solvent type on evaporation

The impact of evaporation was examined using a heated vacuum concentrator (SpeedVac) (Genevac Mivac Duo Concentrator, Genevac Ltd., Ipswich, UK) at 55 °C for

12.5 mM ammonium bicarbonate (AMBIC), 20 mM tris(hydroxymethyl)aminomethane hydrochloride (Tris–HCl) and water as solvents. The evaporation temperature was selected to balance moderate sample decomposition with efficient drying. Evaporation from AMBIC and Tris–HCl solvents was studied as these buffers are commonly used during enzymatic depolymerization. Samples were dissolved in 50 μ L of the specified solvents.

3.2.2. Effect of freezing

Pre-dried samples were dissolved in 50 μ L of water and subjected to repeated freeze-thaw cycles, either for 5 or 10 cycles. Freezing was carried out with standard freezer (–20 °C, freezing time: 1 h) or with liquid nitrogen (–196°C, freezing time: 10 s). Freezing was followed by thawing of samples in a block heater at 37 °C (approximately 1 min), and then after the completion of all freeze-thaw cycles, samples were dried down using SpeedVac.

3.2.3. Effect of storage

Several parameters were investigated that may arise during storage and may have an impact on the recovery of the samples. In the following subsections, the parameters investigated are presented.

To examine the effect of the storage temperature, the samples were stored in 50 μ L water for 48 h at the following temperatures: –18, 4, 20, 37, and 55 °C.

To investigate the effect of storage pH, the pre-dried samples were dissolved in 50 μ L 1 mM hydrochloric acid (pH 3), water (pH 7) and 1 mM NaOH (pH 11). The sample storage was done at 37°C for the following periods: 0, 6, 12 and 24 h.

To examine the effect of the different digestion buffers, the pre-dried disaccharide samples were dissolved in 50 μ L of 12.5 mM AMBIC and 20 mM Tris–HCl. The samples were incubated for 24 and 48 h at 37°C for each buffer.

In order to investigate the impact of storage vessels on the storage stability of HS disaccharide samples, the pre-dried samples were dissolved in 20 μ L water or in a commonly used HPLC–MS injection solvent (10 mM ammonium formate in 75:25 v/v ACN:water). The containers used for the study were 0.5 mL plastic Eppendorf Safe-Lock Tubes (Eppendorf Corporate) and borosilicate type 70 glass vial with glass insert (LAB-EX Kft.). The samples were stored at 4 °C for 24 h to simulate autosampler storage. After storage, all the samples were transferred to plastic tubes for solvent evaporation. In these

experiments, the control samples were mixed, evaporated to dryness and stored dry and frozen in plastic tubes. Before measurement control samples were dissolved in water or injection solvents and dried in new plastic tubes.

To observe the effect of solvents on sample storage stability, pre-dried samples were dissolved in 20 μ L of the examined solvent. The comparison of the following solvents were investigated: 90:10 v/v% ACN:water, 75:25 v/v% ACN:water, 50:50 v/v% ACN:water, 10 mM ammonium formate in 75:25 v/v% ACN:water, 75:25 v/v% MeOH:H2O and 10 mM ammonium formate in 75:25 v/v% MeOH:water. To simulate the autosampler storage all the samples were stored at 4 °C for 0, 6, and 12 h.

3.2.4. HPLC-MS analysis of HS disaccharides in the recovery and stability study

A Waters nano-Acquity ultrahigh performance liquid chromatography (UPLC) system (Waters, Milford, MA, USA) attached to Waters quadruple time of flight (Q-TOF) Premier mass spectrometer (Waters, Milford, MA, USA) was used. The chromatographic separation was carried out on fritted and self-packed, 250 µm i.d. fused silica capillaries. For the fritting of the capillaries a commercial Frit Kit (Next Advance, Inc., Troy, NY, USA) was used. To prepare the frit a 3:1:1 mixture of potassium silicate (Kasil 1624, Kasil 1) and formamide was packed in the capillary, which was dried at 80 °C for 4 h. The separation was performed on GlycanPac AXH-1 (1.9 µm) solid phase (Thermo Fisher Scientific, Waltham, MA, USA), filled into fritted silica capillary by a pressure injection cell in a 10 cm length. For chromatography the following HPLC eluents were used: 10 mM ammonium formate in 75:25 v/v ACN:water (pH 4.4) (solvent A) and 65 mM ammonium formate in 75:25 v/v ACN:water (pH 4.4) (solvent B). For the HS disaccharide chromatographic separation a previously published HPLC–MS method (69) was used, which was the following: isocratic hold on 6% B for 3.5 min, followed by an 0.5 min linear increase up to 70% B and a further linear increase to 95% B in 2.5 min, followed by 3.5 min washing step with 100% B eluent and finally equilibration with 6% B eluent for 5 min. The flow rate was 8 μL/min and the column was thermostat at 45 °C. The MS parameters were chosen as the following: capillary voltage: 1.9 kV; sampling cone voltage: 17 eV, extraction cone voltage: 5 V; source temperature: 80 °C; desolvation temperature: 120 °C; cone gas flow: 25 L/h; desolvation gas flow: 420 L/h. HS disaccharides were detected in negative ionization mode. The detected ions and their m/zvalues are shown in **Table 2**.

3.2.5. Data analysis of the HS disaccharide stability study

The peak area under the curve (AUC) of extracted ion chromatograms (EICs) was integradet by QuanLynx add-in of the Waters MassLynx (4.2) softwar. The data visualization and statistical analysis were conducted using Microsoft Office Excel and Python (3.11.7) with Spyder (5.4.3). First, normality and equality of variance were tested using Shapiro-Wilks- and Levene's-tests. In the case of two group comparisons for equal variance, Student's t-test, for unequal variances, Welch's t-test and for non-normal data Wilcoxon rank sum test were used. For equal variances ANOVA, for unequal variances Welch's ANOVA, and for non-normal data Kruskal–Wallis H-test and the corresponding Tukey HSD, Games-Howell and Dunn post hoc tests were used for multiple group comparisons. The recovery values were illustrated by the relative intensities during the study. Relative intensity values were calculated by dividing the AUC of the corresponding component in the study and the control sample. For data visualization, the average relative intensity values of the parallel samples were used. Data were filtered using median method, except for extreme outliers. In total nine samples were identified to be highly different from their respective replicate samples. In one case, two of the five parallel samples exhibited significant deviations from the rest. Furthermore, samples were classified as outliers if their values differed from the mean of the remaining parallel samples (excluding the outlier) by at least two standard deviations (SDs), either higher or lower. These samples were excluded from further evaluation. The measurement data were submitted to the GlycoPOST database under the accession number GPST000390 (113).

3.3. Analysis of lung tumor sections with different cancer subtypes

The investigation of CS/DS and HS GAGs in different lung tumor subtypes followed the generally used methodology by our research group (**Figure 2**). Each step of the workflow is described in detail in the following subsections.

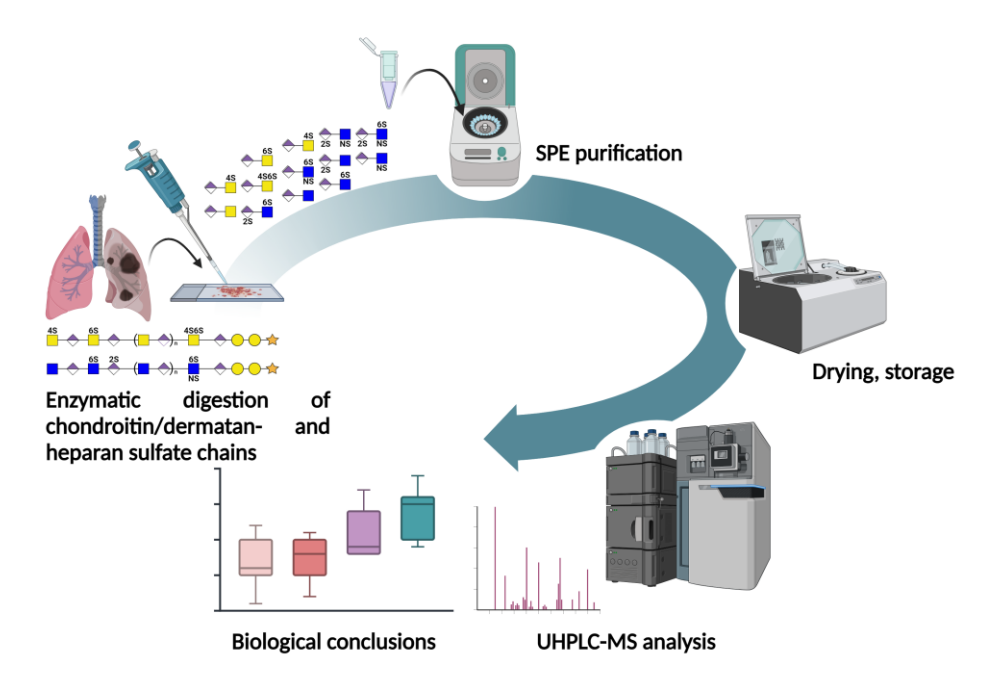


Figure 2. The general workflow of sample preparation and instrumental analysis of CS/DS and HS GAG disaccharides originating from human tissue samples. This figure was created with BioRender.com.

3.3.1. Preparation of lung tissue sections for enzymatic digestion

In this study different LC subtypes and their respective tumor adjacent regions were analyzed. The investigated tissues were formalin-fixed, paraffin-embedded (FFPE) human samples originated from the Department of Pathology, Medical School, and Clinical Center, University of Pécs, and the Teaching Hospital Markusovszky, Szombathely, Hungary. The following LC types were investigated: SCLC and three NSCLC subtypes, AC, SqCC and LCC. The sample cohort was balanced in the study with regards to sex and LC tissue type. The patient data and the histological classification of the samples investigated are detailed in **Table 5.** The most critical part of the applied workflow is the tissue surface digestion of the FFPE tissue samples, as it is difficult to control the size of the digested area. To address this issue, the digested area was circumvented with a razor blade to control the surface area.

Table 5. Detailed summary of the investigated sample groups. HS: cohort for heparan sulfate, CS: cohort for chondroitin- and dermatan sulfate measurements.

	Number of patients	Number of tumor samples	Number of tumor adjacent samples
Total Number	42	81 (CS:41, HS: 40)	72 (CS: 36, HS: 36)
Age	65.5 (54-79)	65.5 (54-79)	65 (54-75)
Male		44	40
CS	22	22	20
HS	22	22	20
Female		37	32
CS	19	19	16
HS	18	18	16
Histology			
Adenocarcinoma		22	18
CS	12	12	9
HS	10	10	9
Large cell carcinoma		20	18
CS	10	10	9
HS	10	10	9
Small cell lung carcinoma		20	20
CS	10	10	10
HS	10	10	10
Squamous cell	10	10	10
carcinoma		19	16
CS	9	9	8
HS	10	10	8

Samples were fixed in 10% buffered formaldehyde and embedded in paraffin. Each piece of tissue was cut into three micrometer-thick sections and stained with hematoxylin-eosin for diagnostic evaluation. Further sections were cut into ten-micrometer-thick pieces that were not stained. For enzymatic digestion, dewaxing is required, which was performed by washing the tissues twice 5 min long with xylene, then 3 min with each 100%, 90% and 70% ethanol, followed by 5 min with 10 mM ammonium bicarbonate and 1 min with water. After dewaxing, to break the cross-linking induced by formalin fixation, antigen retrieval was performed with aqueous solution of 95 mM trisodium citrate and 21 mM citric acid (pH 6). The samples were treated at 85 °C for 30 min. After antigen retrieval, samples were washed with distilled water for 1 min.

3.3.2. Enzymatic digestion of CS/DS GAG chains on tissue surface

The digestion of CS/DS chains was performed using a previously developed methodology with chondroitinase ABC enzyme (70). The composition of the enzyme solution was the

following: 20 mM Tris–HCl, 2.5 mM ammonium acetate, and 2 mU/ μ L chondroitinase ABC (pH = 7.6) and 10% glycerol. The selectivity of chondroitinase ABC towards CS/DS was provided by the used buffer. The enzyme solution was added in 2 μ L droplets in five cycles onto the tissue surface. During the digestion, samples were incubated in a humidified box for 1 h at 37 °C in each cycle, and then a final 24 h of incubation was done. Extraction of the resulting disaccharides was performed with 2 μ L 1% NH₃ solution via 5 cycles of repeated pipetting. The samples were dried in vacuum concentrator (55 °C, approx. 1h) after digestion and stored at –20 °C until further use. The structure and description of Δ 4,5-unsaturated CS/DS disaccharides can be found in **Table 1.**

3.3.3. Enzymatic digestion of HS GAG chains on tissue surface

The digestion of HS chains was also performed based on a previously developed methodology (70). For the digestion a solution of 20 mM Tris–HCl, 2.5 mM Ca(OH)₂, 0.5 mU/ μ L of heparin lyase I, 0.1 mU/ μ L of heparin lyase II, and 0.1 mU/ μ L of heparin lyase III and 10% glycerol was used. During the digestion 2 μ L droplets of the enzyme solution were pipetted onto the surface in three cycles on the first day, then twice on the second day. In each cycle, the samples were incubated in a humidified box at 37 °C, with an additional overnight incubation. Extraction of the resulting disaccharides was performed with 2 μ L 1% NH₃ solution via 5 cycles of repeated pipetting.

3.3.4. GAG disaccharide purification with combined extraction method (cotton wool and graphite solid-phase extraction)

SPE cleanup was performed after digestion to remove salts and other contaminants. The CS/DS and HS disaccharide mixtures were purified using a two-step SPE purification combined clean-up method in order to reduce sample loss. In the first step, the highly polar components (highly sulfated disaccharides) were bound by cotton wool, while the unbound, less polar components that pass through were further purified by graphite SPE. The first step was carried out on cotton wool solid phase in centrifuge pipet tips. The surface activation was performed with 50 μL 60% ACN. Conditioning was done with 50 μL 95% ACN (1% trifluoroacetic acid (TFA)) in two cycles. Samples were applied in 30 μL 95% ACN (1% TFA) and reapplied two times. Salts and contaminants were washed with 50 μL 95% ACN (1% TFA), and then at 37 °C, the CS/DS disaccharides were eluted in two cycles in each with 10 μL, 1% NH₃ solution, while the elution of HS disaccharides

were performed with 10 μ L, 5% NH₃ solvent. The samples were then dried down and stored at -20 °C until further use. The flow-through of the first step underwent a second purification step, where Pierce graphite resin was used in spin columns. The surface activation was done with 100 μ L 80% ACN (1% TFA) in two cycles. Conditioning was done with 100 μ L water in two cycles. Both CS/DS and HS samples were applied in 50 μ L water and incubated 2 minutes before centrifuge. The samples were reapplied. Salts and contaminants were washed with 100 μ L water in three cycles. The disaccharides were eluted in 50 μ L 60% ACN (0.05% TFA) in three cycles. The elution fractions of the first and second steps were combined, then dried down and stored at -20 °C until further use.

3.3.5. HPLC-MS analysis of CS/DS and HS GAG disaccharides

The HPLC-MS measurement of CS/DS was executed by a Waters nanoAcquity UPLC system (Milford, MA, USA) coupled to a Waters Q-Tof Premier mass spectrometer (Milford, MA, USA). The HPLC–MS analysis of HS samples was performed by a Waters Acquity I-class UPLC (Milford, MA, USA) coupled to a Waters Select Series Cyclic Ion Mobility (Milford, MA, USA) mass spectrometer. The chromatographic separation of CS/DS and HS disaccharides was implemented on a self-packed GlycanPac AXH-1 capillary column (250 µm i.d.). For the separation of CS/DS disaccharides, the previously published method (68) was used, while for HS disaccharides, the modified previously shown HPLC-MS method was used. The analysis was performed with the following eluents: 10 mM ammonium formate in 75:25 v/v ACN:water (pH 4.4) (Solvent A) and 65 mM ammonium formate in 75:25 v/v ACN:water (pH 4.4) (Solvent B). For the separation of CS/DS the following 15-min salt gradient was used: start at 6% B and elevate Solvent B to 12% in 0.5 min, then to 60% in 4.5 min, then hold at 100% B for 4 min, and finally equilibrate using the initial composition for 5 min. The flow rate was 8 μL/min and the column thermostat was 45 °C. For the analysis of HS, a 25-min gradient was used, starting from 0% B and holding for 0.1 min, then increasing solvent B to 100% in 0.1 min and holding for 10 min, then reducing solvent B to 0% in 0.5 min and holding for 14.5 min, The flow rate was 8 µL/min and the column was thermostated at 45 °C. The MS instrument parameters were the following: low-flow ESI ion source, the capillary voltage was set to 1.9 kV, the cone voltage was 20 eV, and the desolvation temperature was 120 °C. In the disaccharide measurement, HS disaccharides were observed in MS1 mode, where the trap collision energy was 6 eV and the transfer was 3

eV. The CS/DS was measured in MS1 and MS/MS modes, the mono-sulfated isomer pairs were fragmented with 32 eV to determine the sulfation position. The measurement data were uploaded to the GlycoPOST (ID: GPST000337) database (113).

3.3.6. Data evaluation and interpretation of lung tumor sections with different cancer subtypes

The MS peak integration was performed as written in chapter 3.2.5. Statistical analysis and data visualization were done using R (4.0.5) in RStudio (1.4.1106). For the 4S/6S ratio identification a calibration curve of CS/DS disaccharide standard was used (**Figure 3**). The predominant MS/MS fragment of D0a4 disaccharide is 300.1 m/z, while for D0a6 is 282.1 m/z (114,115). As both fragments are formed for both disaccharides, their intensity ratio is non-linear, calibration requires the use of an exponential curve.

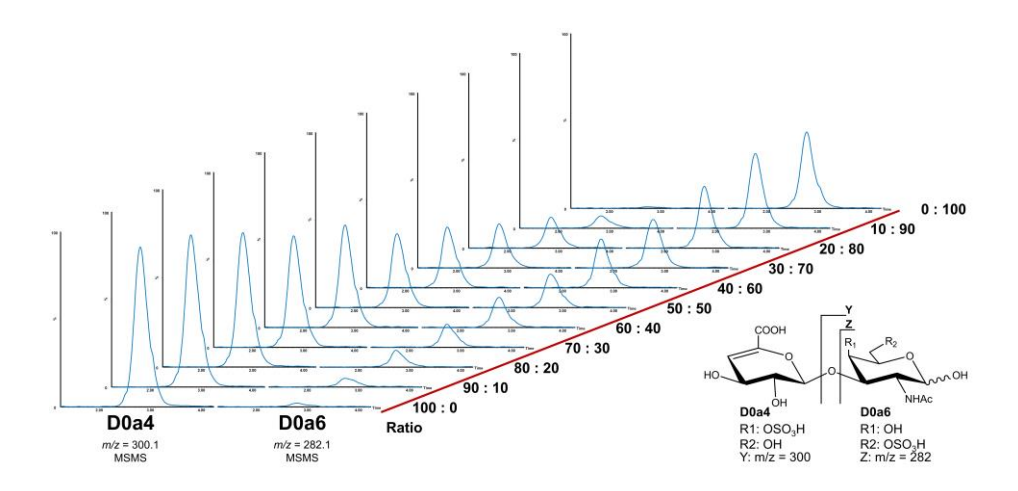


Figure 3. The chromatograms of the D0a4 and D0a6 disaccharide calibration samples through MS/MS fragmentation.

The statistical evaluation process was as follows: normality and equality of variances were assessed using the Shapiro-Wilk test and the Levene's test, respectively, for both multiple and two-group comparisons. For multiple group comparisons, ANOVA, Welch-ANOVA, or Kruskal-Wallis tests were used, while for two-group comparisons, we used Student's *t*-tests, Welch *t*-tests, and Wilcoxon rank sum tests based on the outcomes of the normality and variance equality tests. The Kolgomorov-Smirnov test was used to compare the distribution of HS sample groups. False discovery rates were controlled for all two-group and multiple-group comparisons separately at 5% using the Benjamini-Hochberg method. The gplots package and base R were used to create plots. Principal component analysis was conducted using the prcomp function with variable scaling and

default settings, and hierarchical clustering was performed using the heatmap.2 function with Ward's clustering method "ward.D2" from the helust function.

3.4. Analysis of lung adenocarcinoma sections with different genetic alterations

The workflow used for the analysis of lung tissue samples with different genetic alterations (**Figure 2**) is the same as that described in Section 3.3. Where differences exist, they are indicated separately in the following subsections.

3.4.1. Preparation of lung tissue sections for enzymatic digestion

The investigated FFPE tissue samples were obtained from the National Korányi Institute for Pulmonology. Retrospective FFPE blocks were used for the study. Histological information of the samples investigated is presented in **Table 6**.

Table 6. Clinical characteristics and sample numbers of the investigated lung adenocarcinoma tissue samples.

		Genetic alterations			
		ALK	EGFR	KRAS	WT
Mutation type		-	Exon 18: 6 Exon 19: 13 Exon 20: 2 Exon 21: 8	-	-
Number of	Female	3	17	23	15
patients	Male	5	9	15	9
Age (median)		65 (32-71)	66 (39-79)	63.5 (52-76)	65.5 (41-76)
Grade	Grade 2	7	20	25	13
Grade	Grade 3	1	4	12	11
	Stage 1	2	8	12	5
64	Stage 2	2	13	12	8
Stage	Stage 3	1	5	12	10
	Stage 4	3	-	2	-
	Never	3	8	1	5
Smoking	Former	3	6	14	6
C	Current	_	7	19	12

The preliminary handling of tissue samples before the sample preparation process is the same as described in chapter 3.3.1.

3.4.2. Enzymatic digestion of CS/DS GAG chains

In this case, we used the enzymatic surface digestion method developed previously, but with a different reagent than it was previously described in chapter 3.3.2. (70). The

composition of the used aqueous enzyme solution was the following: 25 mM AMBIC, 2.5 mM ammonium acetate, 2 mU/µL Chondroitinase ABC and 10 % glycerol.

3.4.3. GAG disaccharide purification with combined extraction method (cotton wool and graphite solid-phase extraction)

The SPE purification of the CS/DS disaccharide carried out with the same method as described in chapter 3.3.4.

3.4.4. HPLC-MS analysis of CS/DS GAG disaccharides

The HPLC-MS method for CS/DS disaccharide samples differs slightly from the previously described method in chapter 3.3.5., the differences are highlighted. In this case the investigation was performed by a Waters Acquity I-Class UPLC (Milford, MA, USA) coupled to a Waters Select Series Cyclic Ion Mobility (Milford, MA, USA) MS. The separation was conducted with the previously described column and eluents. The following 15-min salt gradient was used for the elution: 5% B for 7 min, then to 95% B in 5 min, then 95% A in 0.1 min, and hold for 2.9 min as equilibration. The flow rate was 8 μL/min and the column thermostat was 45 °C. The following MS parameters were used: low-flow ESI ion source, the capillary voltage was set to 2.5 kV, the cone voltage was 10 eV, and the temperature was 120 °C. CS/DS disaccharides were analyzed in MS1 and MS/MS mode, where the trap collision energy was 6 eV and the transfer was 4 eV, the mono-sulfated isomer pairs were fragmented with 20 eV. The measurement data is uploaded to GlycoPOST database (ID: GPST000547) (113).

3.4.5. Data evaluation

The chromatographic peak integration was done as previously described in section 3.2.5. and 3.3.6. The statistical analysis and visualization of the data were performed similarly, but different in many ways from chapter 3.2.5., therefore it is explained in detail. The used software for statistical analysis and visualization were Microsoft Office Excel and Python (3.11.7) with Spyder (5.4.3). Hierarchical clustering analysis was done by Scipy (1.13.1.) package, the PCA and its visualization was created with Scikit-learn (1.4.2.), The boxplots were created by Matplotlib (3.8.4.) and Seaborn (0.13.2.) packages. The statistical analysis was performed with following method: the investigation of the data normality and equality of variance was performed with Shapiro-Wilk normality-and Levene's test. Based on the results of the normality and equality of variance tests, multiple group comparisons were performed with the appropriate statistical tests which were the

following: ANOVA, Welch-ANOVA, or Kruskal-Wallis tests. In the case of significant results, the corresponding post hoc test were done (Tukey HSD, Gams-Howell, Dunn's test) to identify the differed groups. Statistical tests were performed beside α =0.05 value. The false discovery rate was controlled at 5% during the statistical analysis using the Benjamini-Hochberg method for the multiple group comparison results and in the case of those post-hoc test when it was required (Tukey HSD, Dunn's test). In cases where the concentration values calculated with the calibration curves were negative, these values were considered as " θ " as a negligible value.

4. Results

4.1. Stability studies of HS disaccharides

A typical sample preparation workflow of GAG disaccharides from tissues includes extraction and digestion of polysaccharide chains into disaccharides, derivatization (optional), sample clean-up and instrumental analysis (**Figure 4**, left panel). This multistep sample preparation process requires several intermediate sample handling steps, which can significantly affect the intensity values obtained during measurements (**Figure 4**, right panel). We thoroughly examined these steps, including storage in digestion buffers, sample purification and injection, as well as solvent evaporation and freezing cycles for preservation. Additional sample handling steps affecting stability and recovery were also considered and are discussed further. Although our comparisons were based on small sample sizes, several cases showed only trends that were often not statistically significant. We also identified several cases with statistically significant differences, confirmed through statistical tests.

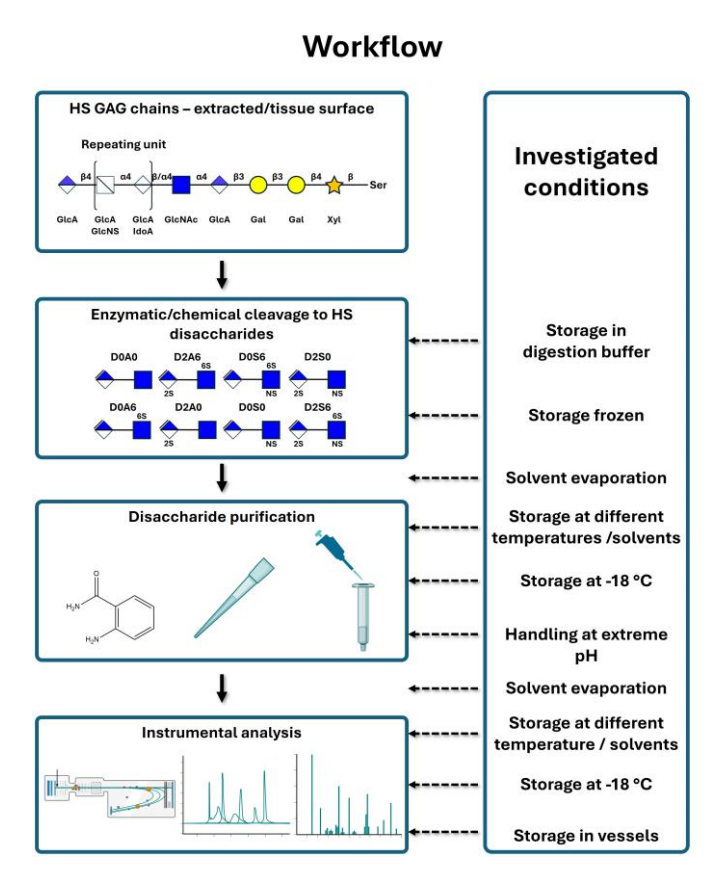


Figure 4. Generally used workflow of sample preparation and analytical measurement of heparan sulfate. On the right panel, the investigated sample preparation conditions are listed such as solvent evaporation and storage conditions. Dashed arrows highlight the points in the general workflow where the corresponding sample handling step is applied. Part of this figure was created with BioRender.com.

Throughout the stability study of HS disaccharides, under dissociation, we refer to sulfate group loss in the ion source, which can be easily identified in the HPLC–MS EICs. Meanwhile, degradation occurs during sample preparation and storage, which cannot be distinguished by chromatography, and can only be determined by comparing intensity values with control sample.

4.1.1. Effect of solvent type on evaporation

First, the impact of the solvent on the vacuum centrifugal evaporation process was investigated. The results suggested that the used solvents strongly influenced the recovery of the samples (**Figure 5A**). For most HS disaccharides, recovery rates ranged between 80% and 100% using either 12.5 mM AMBIC or water as solvent. In some cases, recovery values exceeded 100% (AMBIC: D0S0, D2A6 and D0S6; water: D0S0 and D2A6), though these variations remained within the standard deviation (SD) of technical replicates. Based on the SD values, evaporation from water proved to be more favorable than AMBIC.

Examining the effect of evaporation from 20 mM Tris-HCl, a drastic reduction was observed in the sample content. Investigating the EICs of the HS disaccharides, significant peak frontings were identified, but the peak maximum was located at the same retention time as in the control samples (**Figure 5B**). Presumably the products were decomposed during electrospray ionization, as it was not possible to identify any changes in the mass spectrum. As a result, no relative intensity values were defined for this solvent.

4.1.2. Effect of freezing

Freezing and thawing cycles of the standard samples were modeled, as these samples are typically stored frozen in bulk but must be thawed repeatedly for use and then refrozen for continued storage. Consequently, it is crucial to investigate the effect of the freezing method and the number of freezing cycles. In this study commonly used freezing methods (-20 °C freezer and -196 °C liquid nitrogen) were examined in 5 and 10 cycles. Several differences were identified between the two methods and the number of cycles (**Figure 5C**). In the case of five cycles storage, the disaccharide content was lower in the -20 °C freezer. The SD was not significantly different among the two methods except for D0S6 disaccharide, which had 4.5 times higher SD in liquid nitrogen. Comparing 10-cycle freezing, samples stored in the freezer showed higher average recovery (80%–95%)

than those frozen in liquid nitrogen (70%–90%), however the SD was twice as high in the case of freezer.

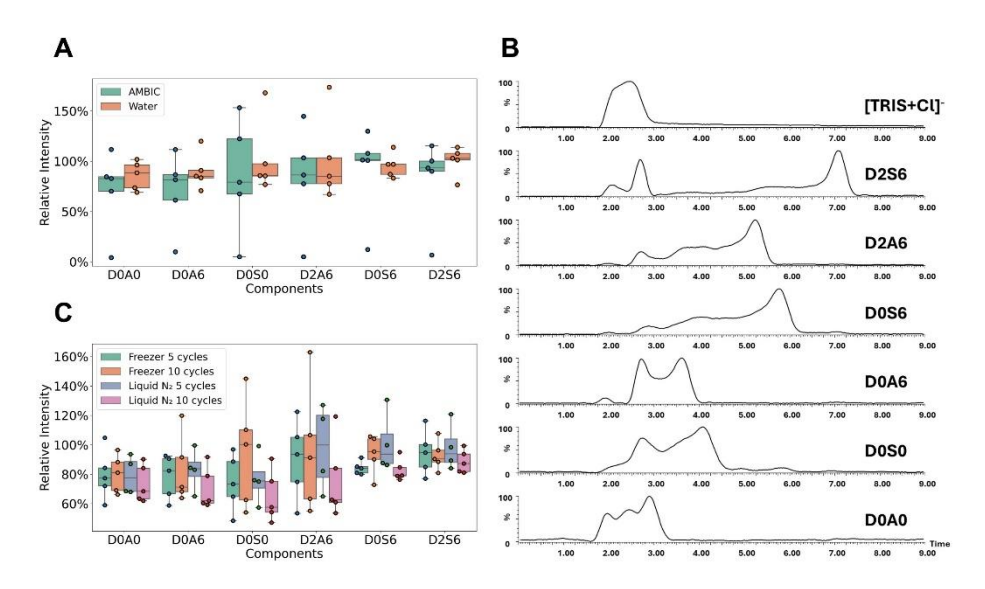


Figure 5. Effects of evaporation and freezing. (A) Recovery values after evaporation in a heated vacuum centrifuge in the case of 12.5 mM ammonium bicarbonate (AMBIC) and water, (B) EICs of Tris–HCl and the six measured HS disaccharides during the evaporation experiment. ([Tris+Cl]– is the chloride adduct ion of Tris), (C) recovery values after 5 and 10 cycles of freezing and thawing with freezer (freezer) or liquid nitrogen (liquid N2). In parts (A) and (C), the recovery values are compared to the control samples (relative intensity). Average n = 5 samples were measured in the groups except in cases that were excluded as defined in Section 3.2.5.

4.1.3. Effect of storage

To minimize the sample loss, it is essential to choose the right storage parameters. Therefore, the following parameters were investigated: storage temperature, pH, digestion buffer and type of solvents.

The effect of storage temperature was investigated for aqueous solutions, which were stored for 48 h at -18, 4, 20, 37, and 55 °C. The results indicate that storing samples at or below 4 °C for 48 h is a viable option, as disaccharide recovery at -18 and 4 °C ranged between 85% and 95% (**Figure 6**). At 20 °C, recovery ranged from 80% to 100%, however the SD was four times higher than at 4 °C. At higher temperatures (37 and 55 °C), the recovery decreased, while the SD generally increased, particularly for the D0S0 disaccharide.

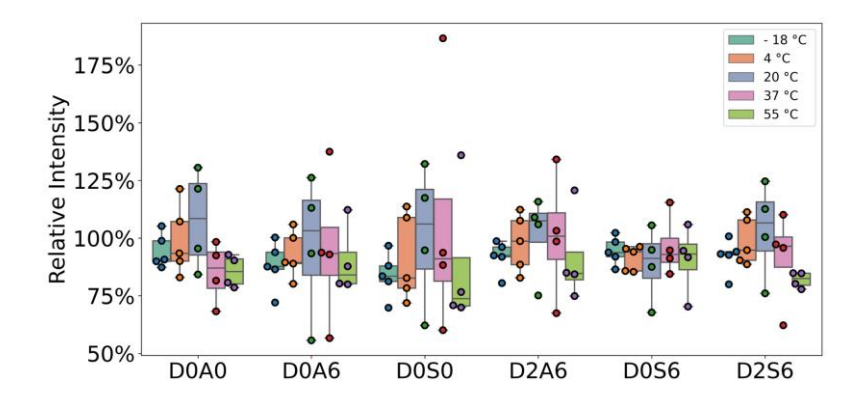


Figure 6. Effect of -18, 4, 20, 37 and 55 °C temperatures for 48 h storage. HS samples were stored in water in plastic tubes (Eppendorf Safe-Lock Tubes). (* p < 0.05; ** p < 0.01 and *** p < 0.001).

Sulfated HS disaccharides have negative charge and these sulfate groups can be easily cleaved off the disaccharides, which can be significantly affected by the pH of the solvent. To investigate the effect of different pH values on the stability of HS disaccharides, the samples were stored in 1 mM hydrochloric acid (pH 1), MilliQ water (pH 7) and 1 mM sodium hydroxide (pH 11) solvents at 37°C for 0, 6, 12 and 24 h (**Figure 7**). The most significant sample loss occurred at basic pH (pH 11), with recovery values ranging between 10% and 60% (**Figure 7**). At pH 3, recovery ranged from 60% to 100%. In acidic conditions, sample recovery was significantly higher than at basic pH, though the SD values remained similar. Under neutral conditions (pH 7), recovery varied between 75% and 100%.

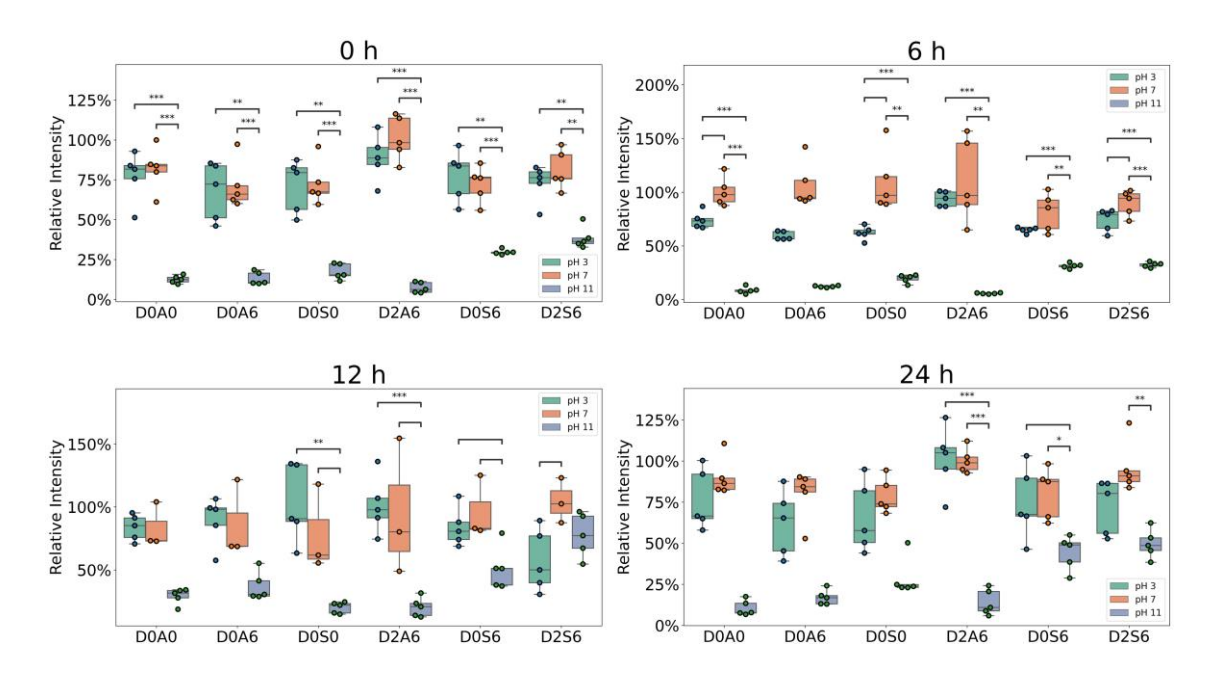


Figure 7. Effect of sample storage under pH 3, 7 and 11 for 0, 6, 12 and 24 h in water. HS samples were stored in plastic tubes (Eppendorf Safe-Lock Tubes). (* p < 0.05; ** p < 0.01 and *** p < 0.001).

Several significant differences were identified between pH 3 and 11, as well as between pH 7 and 11. All the significant differences are shown in **Table 7**. The observations indicate minor differences between recoveries across storage durations; however, these variations fall within the SD. This suggests that the recovery of the samples was influenced heavily by the storage pH.

 Table 7. Summary of significant changes identified during storage under different pH conditions.

Storage time	Compound	Compared groups	Number of samples (in groups)	Statistical test	Post hoc test	p-value	The degree of deviation (fold change)
	D040	pH 11 – pH 3	5 – 5	ANOVA	Tukey HSD	< 10-8	0.1619
	D0A0	pH 11 – pH 7	5 – 5	ANOVA	Tukey HSD	< 10-8	0.1524
	D0A6	pH 11 – pH 3	5 – 5	ANOVA	Tukey HSD	0.0001	0.1936
	DOAG	pH 11 – pH 7	5 – 5	ANOVA	Tukey HSD	0.0001	0.1835
	D0S0	pH 11 – pH 3	5-5	ANOVA	Tukey HSD	0.0001	0.2438
0 h	D030	pH 11 – pH 7	5 - 5	ANOVA	Tukey HSD	0.0001	0.2389
V II	D2A6	pH 11 – pH 3	5 – 5	ANOVA	Tukey HSD	< 10 ⁻⁸	0.0821
	DZAO	pH 11 – pH 7	5 – 5	ANOVA	Tukey HSD	< 10 ⁻⁸	0.0722
	D0S6	pH 11 – pH 3	5 - 5	ANOVA	Tukey HSD	0.0001	0.3817
	D050	pH 11 – pH 7	5 – 5	ANOVA	Tukey HSD	0.0002	0.4110
	D2S6	pH 11 – pH 3	5 – 5	ANOVA	Tukey HSD	0.0007	0.5285
	D250	pH 11 – pH 7	5 – 5	ANOVA	Tukey HSD	0.0001	0.4754
	D0A0 D0S0	pH 11 – pH 3	5 – 5	ANOVA	Tukey HSD	< 10 ⁻⁸	0.1164
		pH 11 – pH 7	5 – 5	ANOVA	Tukey HSD	< 10 ⁻⁸	0.0859
		pH 11 – pH 3	5 – 5	ANOVA	Tukey HSD	0.0053	0.3152
		pH 11 – pH 7	5 – 5	ANOVA	Tukey HSD	< 0.0001	0.1782
	D2A6	pH 11 – pH 3	5 – 5	Welch's ANOVA	Games- Howell	< 0.0001	0.0609
6 h		pH 11 – pH 7	5 – 5	Welch's ANOVA	Games- Howell	0.0086	0.0517
	D0S6	pH 11 – pH 3	5 – 5	Welch's ANOVA	Games- Howell	< 10 ⁻⁷	0.4844
		pH 11 – pH 7	5 – 5	Welch's ANOVA	Games- Howell	0.0066	0.3852
		pH 11 – pH 3	5 – 5	ANOVA	Tukey HSD	< 10 ⁻⁸	0.4393
		pH 11 – pH 7	5 – 5	ANOVA	Tukey HSD	< 10 ⁻⁸	0.3611
	D0S0	pH 11 – pH 3	5 – 5	ANOVA	Tukey HSD	0.0011	0.1969
		pH 11 – pH 7	5 – 5	ANOVA	Tukey HSD	0.0242	0.2562
	D2A6	pH 11 – pH 3	5 – 5	ANOVA	Tukey HSD	0.0031	0.2019
12 h		pH 11 – pH 7	5 – 5	ANOVA	Tukey HSD	0.0134	0.2163
	D0S6	pH 11 – pH 3	5 – 5	ANOVA	Tukey HSD	0.0436	0.6112
		pH 11 – pH 7	5 – 5	ANOVA	Tukey HSD	0.0175	0.5400
	D2S6	pH 7– pH 3	5 – 5	ANOVA	Tukey HSD	0.0278	1.8219
	D2A6	pH 11 – pH 3	5 – 5	ANOVA	Tukey HSD	< 10 ⁻⁸	0.1393
		pH 11 – pH 7	5 – 5	ANOVA	Tukey HSD	< 10-8	0.1409
24 h	D0S6	pH 11 – pH 3	5 – 5	ANOVA	Tukey HSD	0.0357	0.5940
		pH 11 – pH 7	5 – 5	ANOVA	Tukey HSD	0.0130	0.5499
	D2S6	pH 11 – pH 7	5 – 5	ANOVA	Tukey HSD	0.0006	0.5179

Since in most cases HS disaccharides are analyzed from biological origin, it is important to investigate the effect of the most commonly used digestion buffers during enzymatic cleavage on sample recovery taking into account the possible digestion times, which is up to 48 h. AMBIC or Tris–HCl buffers are generally used for the depolymerization of the HS chains (22,35,79). Stabilities of HS disaccharides were examined during 24 and 48 h storage in AMBIC solution at 37 °C (**Figure 8**). The recovery was between 70% and 100%. Comparing the 24 h and 48 h storage, disaccharide content and the SD were higher at 24 h. After 48 h, recovery decreased for most disaccharides, except for D2A6 and D0A0, which showed an increase, with a relative SD of 26%. The recovery of most disaccharides dropped significantly after 24 and 48 h storage in 20 mM Tris–HCl solvent.

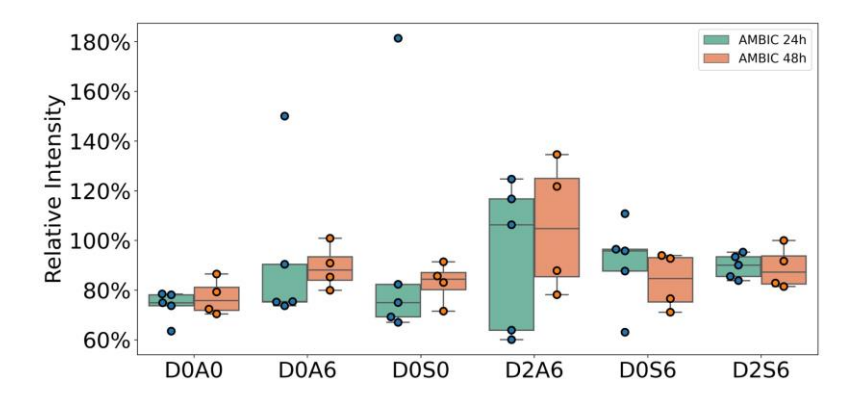


Figure 8. Effect of sample storage in 12.5 mM AMBIC digestion solvent for 24 and 48 h (AMBIC: ammonium bicarbonate). HS samples were stored in water in plastic tubes (Eppendorf Safe-Lock Tubes). (* p < 0.05; ** p < 0.01 and *** p < 0.001).

phenomenon previously observed the same as mentioned chapter 4.1.1. during evaporation from Tris-HCl. Fronting chromatographic peaks (Figure 9) and a drastic decrease in abundances were also observed. To investigate the phenomenon in detail, further investigation was performed. First, pure Tris-HCl buffer was injected, followed by co-injection of 20 mM Tris-HCl with HS disaccharides. During the pure Tris-HCl injection, Tris eluted from the chromatography column in its chloride adduct form ([Tris+Cl]⁻) at the dead time, indicating that it is not responsible for fronting and does not contribute to ion suppression during the MS measurements. Next, HS standard disaccharide samples were dissolved in 20 mM Tris-HCl buffer and measured by the HPLC-MS method before (Figure 9A) as well as after storage at 37 °C for 24 h (Figure 9B). There were no visible differences in the chromatography between the two measurements. Finally, evaporation was performed for 10 and 50 μL volumes of 20 mM

Tris–HCl buffer. After evaporation, the samples were re-dissolved in the injection solvent. The evaporation time (and thus the length of the incubation of the sample at 55 °C) was 50 min for the $10~\mu L$ volume, whereas 140 min for the $50~\mu L$ samples. The fronting was not observed in the case of evaporation from $10~\mu L$ Tris–HCl buffer (**Figure 9C**), however, the fronting was repeatable when the evaporation was performed from $50~\mu L$ Tris–HCl buffer (**Figure 9D**). The phenomenon could not be observed during co-injection of HS disaccharides and TRIS-HCl solutions, neither after the evaporation from $10~\mu L$ TRIS-HCl, but it was reproducible after evaporation from $50~\mu L$ TRIS-HCl (Figure 9). This indicates that a chemical interaction between Tris and the HS disaccharides occurs at 55° C after a longer period, these conditions are not the same as for enzymatic digestion.

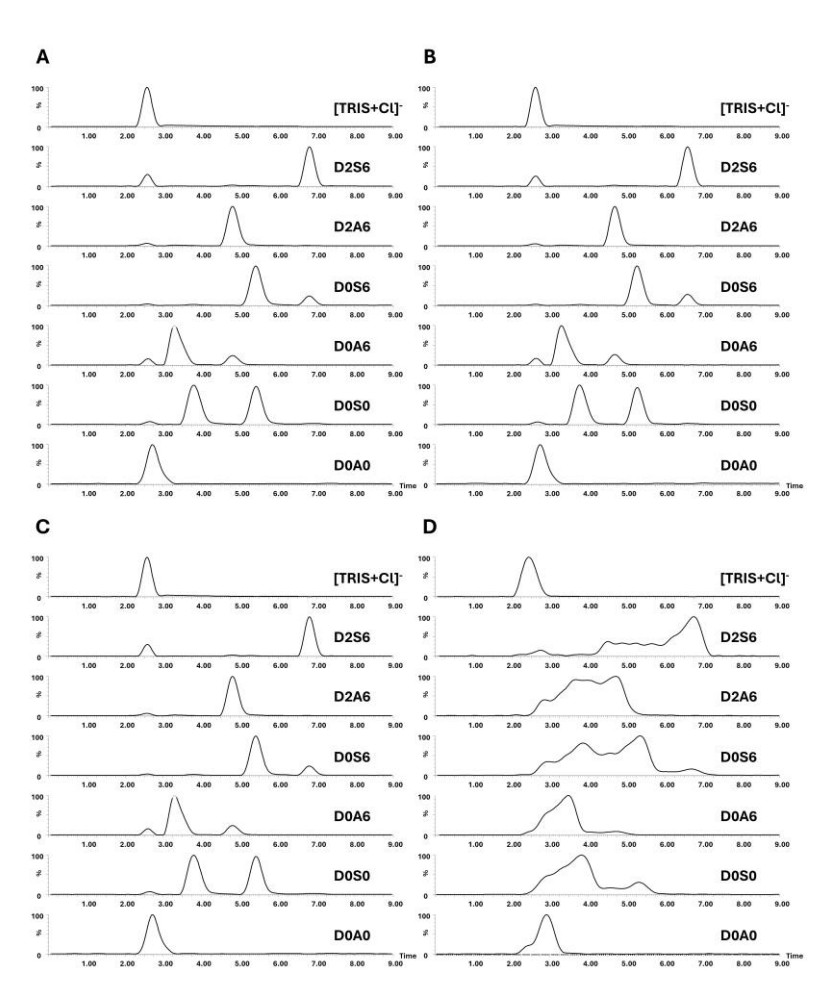


Figure 9. Extracted ion chromatograms of TRIS-HCl and the 6 investigated disaccharides A: HS standards injected directly from TRIS-HCl without storage, B: HS standards stored in TRIS-HCl at 37 °C for 24 hours, C: HS standards dried from 10 μ L TRIS- HCl and injected from injection solvent, D: HS standards dried from 50 μ L TRIS-HCl and injected from injection solvent.

It was important to investigate the HS disaccharides stored in commonly used plastic tubes and glass vials with insert, because charged molecules such as the HS disaccharides can irreversibly adsorb on the surface of the containers wall (**Figure 10**). Comparison was also made between storing samples in water or the HPLC–MS injection solvent for both storage vessels. For aqueous solutions higher recovery values were observed in plastic tubes. Examining the glass vial, using water as solvent higher recoveries with smaller SD values were observed for most disaccharides except for D2S6. In glass vial the D0S6 and D2S6 disaccharides showed a significantly higher recovery in water (with 1.36 and 1.38fold) than in the injection solvent (**Figure 10**).

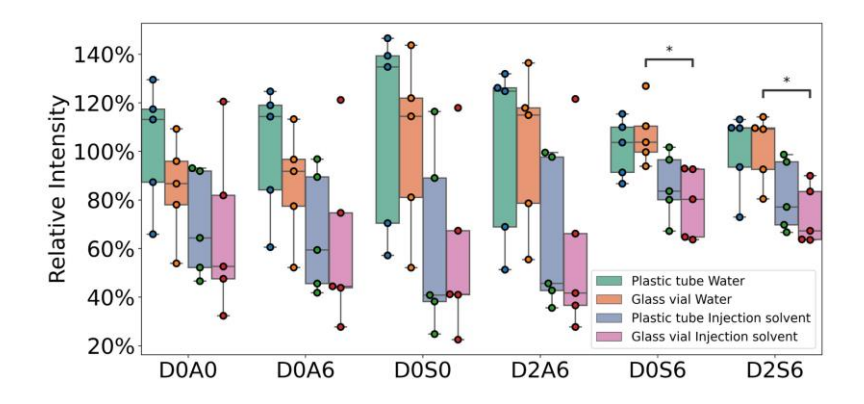


Figure 10. Effect of sample storage in different storage vessels. HS samples were stored in water and in the injection solvent in plastic tubes (Eppendorf Safe-Lock Tubes) or in glass vials with insert. (* p < 0.05; ** p < 0.01 and *** p < 0.001).

The choice of chromatography system, and the analytes investigated determines the applicable eluents and injection solvents. In addition to the requirements of the system, the potential degradation of the samples must also be considered as discussed earlier. The most commonly used injection solvents for disaccharide analysis are water, ACN, MeOH and their mixtures with or without buffer salts.

The effect of the injection solvents on the recovery of HS disaccharide samples during storage at 4°C for 0, 6 and 12 h were examined (**Figure 11**). Considering both the recovery and variance values, the ACN-based solvents (solvents a, b, c and d) provided more reliable results over 12 h storage (except the 75:25 ACN:water solvent), compared to the MeOH–containing solvents (solvents e and f). In the case of total disaccharide content, the lowest recovery for ACN solvents was observed for 75:25 ACN:water ratio (solvent b). The 90:10 ACN:water ratio (solvent a) demonstrated higher recovery and lower SD, except for D0A0 and D0S6 disaccharides, compared to other ACN ratios. In

the presence of 10 mM ammonium formate (solvent d) recovery increased, while the SD decreased for the highly sulfated D0S6 and D2S6 disaccharides. For MeOH containing solvents (solvents e and f), the added salt increased the recovery for most disaccharides by approximately 30% after 6 and 12 h storage, but the SD also increased for almost all disaccharides.

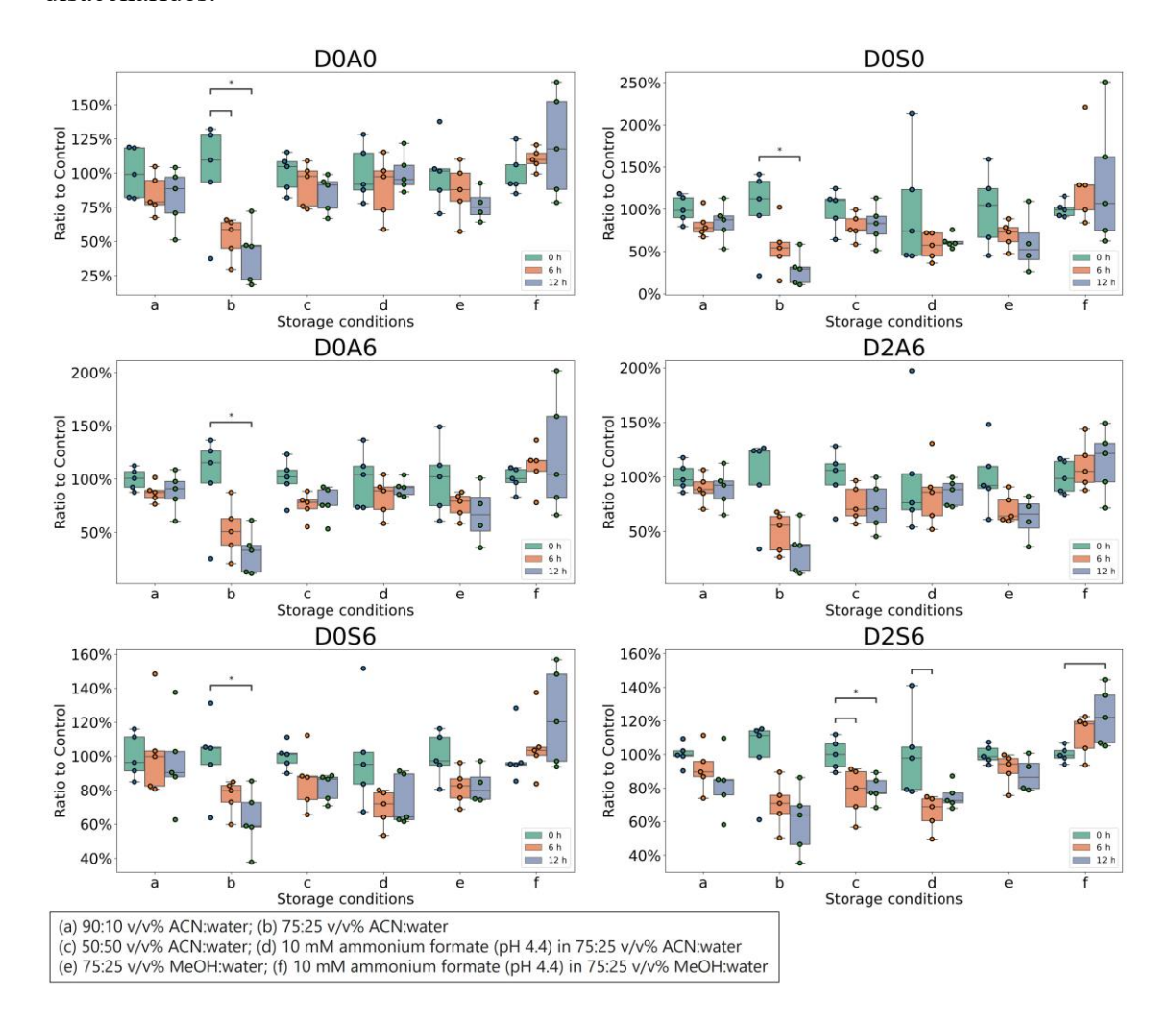


Figure 11. Relative recovery values during the storage of HS disaccharides for 0, 6 and 12 h at 4°C in different solvents. (a) 90:10 v/v% acetonitrile (ACN):water; (b) 75:25 v/v% ACN:water; (c) 50:50 v/v% ACN:water; (d) 10 mM ammonium formate (pH 4.4) in 75:25 v/v% ACN:water; (e) 75:25 v/v% methanol (MeOH):water; (f) 10 mM ammonium formate (pH 4.4) in 75:25 v/v% MeOH:water. (*: p < 0.05). Average n = 5 samples were measured in the groups.

Table 8. Summary of significant changes identified during storage in different injection solvents.

Storage solvent	Compound	Compared groups	Number of samples (in groups)	Statistical test	Post hoc test	p-value	The degree of deviation (fold change)
	D0A0	0 h - 6 h	5 – 5	ANOVA	Tukey HSD	0.0407	0.5257
	DUAU	$0\ h-12\ h$	5 – 5	ANOVA	Tukey HSD	0.0124	0.4124
75:25 v/v% ACN:water	D0A6	$0\ h-12\ h$	5 - 5	ANOVA	Tukey HSD	0.0130	0.3136
	D0S0	$0\ h-12\ h$	5 - 5	ANOVA	Tukey HSD	0.0183	0.2851
	D0S6	0 h - 12 h	5 - 5	ANOVA	Tukey HSD	0.0186	0.6259
50.50 / 0/ A CNI	D2S6	0 h - 6 h	5 - 5	ANOVA	Tukey HSD	0.0174	0.7730
50:50 v/v% ACN:water		0 h - 12 h	5 – 5	ANOVA	Tukey HSD	0.0278	0.7912
10 mM ammonium formate (pH 4.4) in 75:25 v/v% ACN:water	D2S6	0 h – 6 h	5 – 5	ANOVA	Tukey HSD	0.0161	0.6544
10 mM ammonium formate (pH 4.4) in 75:25 v/v% MeOH:water	D2S6	0 h – 12 h	5 – 5	ANOVA	Tukey HSD	0.0355	1.2271

All the investigated conditions and the identified optimal and non-optimal parameters in the HS stability and recovery study are summarized in **Table 9**.

Table 9. The investigated parameters in each sample preparation step and the conditions considered optimal and avoidable.

Step	Tested	Effect	Optimal	Non-optimal	
Storage – digestion buffer	12.5 mM AMBIC 20 mM TRIS-HCl 24; 48 hours storage	No direct effect but subsequent evaporation has strong effect on chemical stability	12.5 mM AMBIC	20 mM TRIS-HCl	
Evaporation from digestion buffer or long-term storage solution	12.5 mM AMBIC Water 20 mM TRIS-HCl	Strong effect on chemical stability	12.5 mM AMBIC water (best)	20 mM TRIS-HCl	
Storage - temperature	-18; 4; 20; 37; 55 °C	Strong effect on repeatability of recoveries	-18; 4 °C	20; 37; 55 °C	
Storage - pH	pH = 3 (1 mM HCl) pH = 7 (water) pH = 11 (1 mM NaOH) 0; 6; 12; 24 hours storage	Strong effect of pH on chemical stability Minor effect of storage time on repeatability of recoveries	pH = 3 (best) $pH = 7$	pH = 11	
Freezing - method	-20 °C (freezer) -196 °C (liquid nitrogen)	No difference	-20 °C (freezer) -196 °C (liquid nitrogen)		
Freezing - cycles	5 or 10 cycles	Small difference	5 cycles	10 cycles	
Storage – injection	90:10 v/v% ACN:water 75:25 v/v% ACN:water 50:50 v/v% ACN:water 1 mM ammonium formate	Major differences based on	90:10 v/v% ACN:water 10 mM ammonium formate (pH 4.4) in	75:25v/v% ACN:water	
storage – Injection solvent	in 75:25 v/v% ACN:water 75:25 v/v% MeOH:water 1 mM ammonium formate in 75:25 v/v% MeOH:water 0; 6; 12; 24 hours storage	sulphation type (N/O) and the solvent used	75:25 v/v% MeOH:water 10 mM ammonium formate in 75:25 v/v% ACN:water	50:50 v/v% ACN:water 75:25v/v% MeOH:water	

4.2. Analysis of lung tumor sections with different cancer subtypes

In this study CS/DS and HS chains were investigated from FFPE lung tissue. The samples were derived from various LC subtypes (AC, SqCC, LCC, and SCLC) and tumor adjacent normal tissue regions. Altogether 77 CS/DS (41 tumor, 36 tumor adjacent normal) and 76 HS (40 tumor, 36 tumor adjacent normal) samples were investigated. The sample and patient information are summarized in **Table 5**. The results are based on the specified sample numbers; slight variations may occur in some cases due to missing data. For the calculation of the total *N/O* ratio, missing values were considered as zeros. The alterations in CS/DS and HS GAGs were examined at the disaccharide level.

Principal component analysis (PCA) was performed independently for the identified CS/DS and HS disaccharides (**Figure 12**) to determine whether variations in disaccharide abundance could differentiate tumor samples from tumor-adjacent tissues, as well as distinguish the different lung cancer phenotypes. For CS/DS (**Figure 12**), the tumor and tumor adjacent samples are slightly better separated than for HS (**Figure 12**), which could not be distinguished based on the quantity of HS disaccharides with high degree of confidence. Furthermore, PCA results showed that lung cancer subtypes were not differentiated from each other considering the abundance of CS/DS and HS disaccharides.

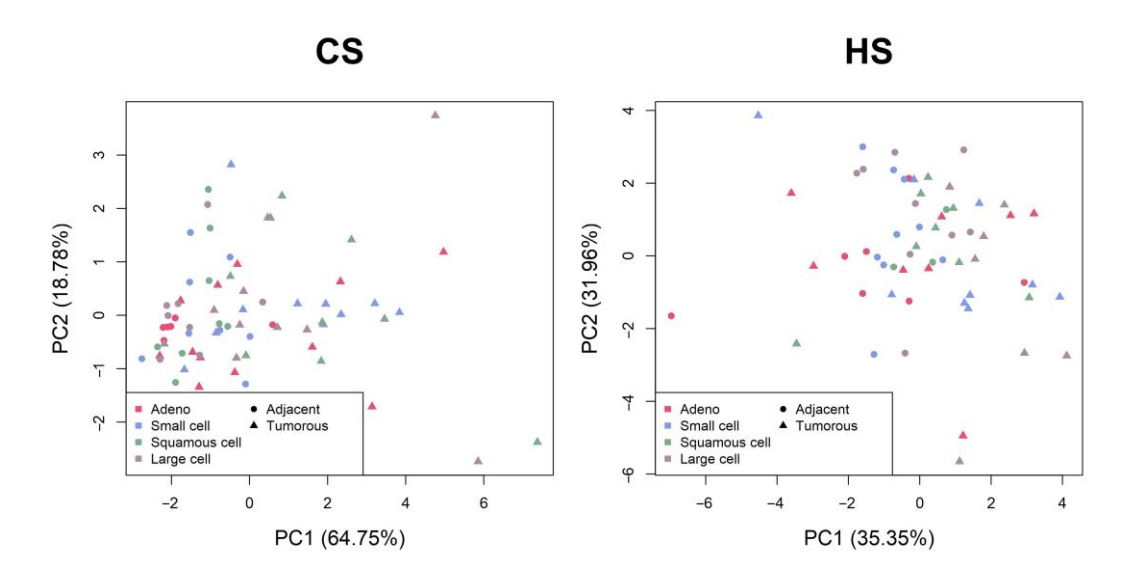


Figure 12. PCA of the investigated CS/DS and HS samples. The disaccharide abundances were used for plot. Triangles and circles indicate tumor and tumor-adjacent samples, respectively. The different colors mark the different sample groups (pink for AC, blue for SCLC, green for SqCC, and grey for LCC).

4.2.1. CS/DS and HS quantity and sulfation characteristics between all tumor and all tumor adjacent normal samples

Total CS/DS disaccharide quantity was found to be significantly higher in the tumor tissue samples compared to adjacent samples (**Figure 13**). Examining the individual CS/DS disaccharides between all the tumor and adjacent sample groups, significant differences were observed in the D0a0, D0a4, and D0a6 disaccharide content (**Figure 13**). In the tumor samples the D0a0 abundance decreased, while the D0a4 and D0a6 content increased. The doubly sulfated D0a10 disaccharide was present in low abundance and did not show significant differences between any of the sample groups.

The sulfation patterns were examined to identify the structural changes in GAGs. CS/DS sulfation changed significantly between all tumor and all adjacent tissue samples, in the case of average degree of sulfation and the 6-O/4-O-sulfation ratio (**Figure 13**). In the tumor samples the average degree of sulfation was found to be higher, while the 6-O-/4-O-sulfation ratio was lower. The significant statistical results of CS/DS characteristics between all adjacent and all tumor samples are highlighted in **Table 10**.

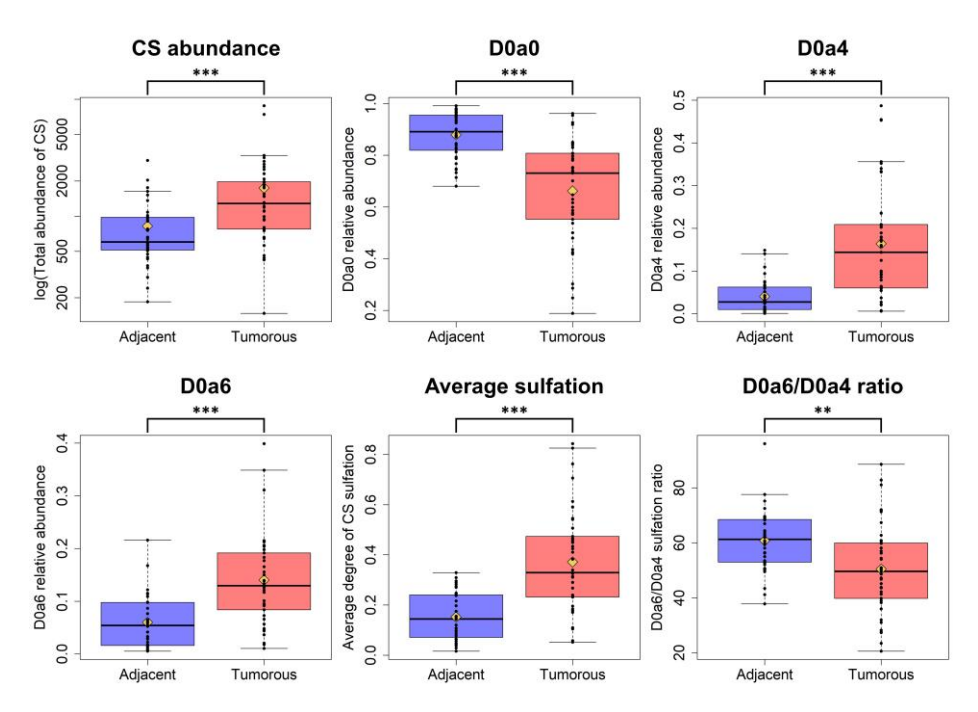


Figure 13. Box plots of significant CS/DS characteristics between all adjacent and all tumor samples. The yellow diamonds indicate the average values of the respective sample groups. (**: p < 0.01; ***: p < 0.001).

Table 10. Summary of significant changes identified during the examination of CS/DS characteristics between all adjacent and all tumor samples.

Compared sample groups	Aspect of comparison	Number of tumor samples	Number of tumor adjacent samples	Statistical test	p-value	The degree of deviation (fold change)
	Total quantity	41	36	Wilcoxon	<10-4	2.212
	D0a0 quantity	41	36	Wilcoxon	<10-6	0.753
All tumor	D0a4 quantity	41	32	Wilcoxon	<10-6	4.057
	D0a6 quantity	41	32	Wilcoxon	<10-5	2.331
and all adjacent	Average sulfation	41	36	Wilcoxon	<10-6	2.443
	D0a6/D0a4- sulfation ratio	41	36	Student t	<10-2	0.830

The total HS disaccharide content showed almost identical values both in tumor and tumor-adjacent regions. This similarity was tested with Kolgomorov-Smirnov test (p = 0.9959). Comparing all the tumor and all the tumor-adjacent samples, significant changes were observed in the abundance of the D2A0 + D0A6 and D2S0 + D0S6 HS disaccharides (**Figure 14**). The relative quantity of D2A0 + D0A6 was higher, while it was lower for D2S0 + D0S6 in the tumor samples. Examining the HS sulfation between the tumor and adjacent samples, a decrease of the mono-, di-, and total N/O-sulfation ratios were identified in the case of the tumor samples (**Figure 14**). The significant statistical results of HS characteristics between all adjacent and all tumor samples are highlighted in **Table 11**.

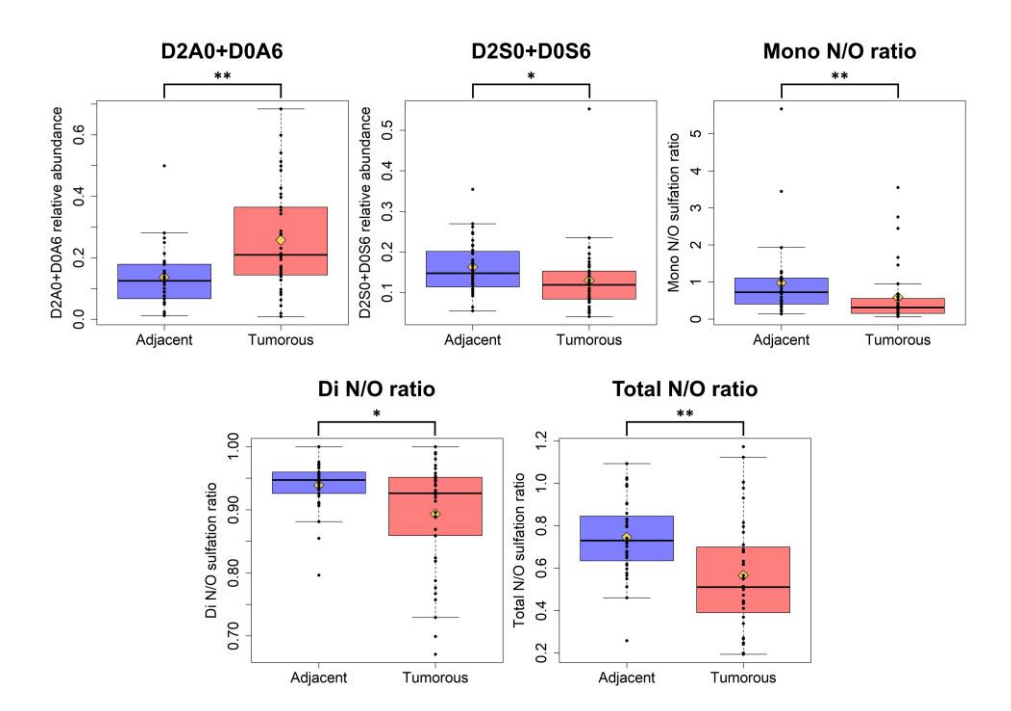


Figure 14. Box plots show significant differences in HS characteristics between all adjacent and all tumor samples. Mono-, di-, and total N/O-sulfation ratios were calculated as the ratio of the corresponding disaccharides weighted by their contribution to O- and N-sulfation (the number of the respective sulfate groups on each disaccharide). The yellow diamonds indicate the average values of the respective sample groups. (*: p < 0.05; **: p < 0.01).

Table 11. Summary of significant changes identified during the examination of HS characteristics between all adjacent and all tumor samples.

Compared sample groups	Aspect of comparison	Number of tumor samples	Number of tumor adjacent samples	Statistical test	p-value	The degree of deviation (fold change)
All tumor and all adjacent	D2A0+D0A6 quantity	37	31	Wilcoxon	<10-2	1.886
	D2S0+D0S6 quantity	40	36	Wilcoxon	< 0.05	0.796
	Mono <i>N/O</i> -sulfation	36	31	Wilcoxon	<10-2	0.599
	Di N/O-sulfation	40	36	Wilcoxon	< 0.05	0.952
	Total N/O-sulfation	40	36	Student t	<10-2	0.759

Examining the hierarchical clustering of tumor and tumor-adjacent samples, the results showed that in the case of CS/DS, several tumor samples clustered together, while in the case of HS, no co-clustering was observed (**Figure 15**).

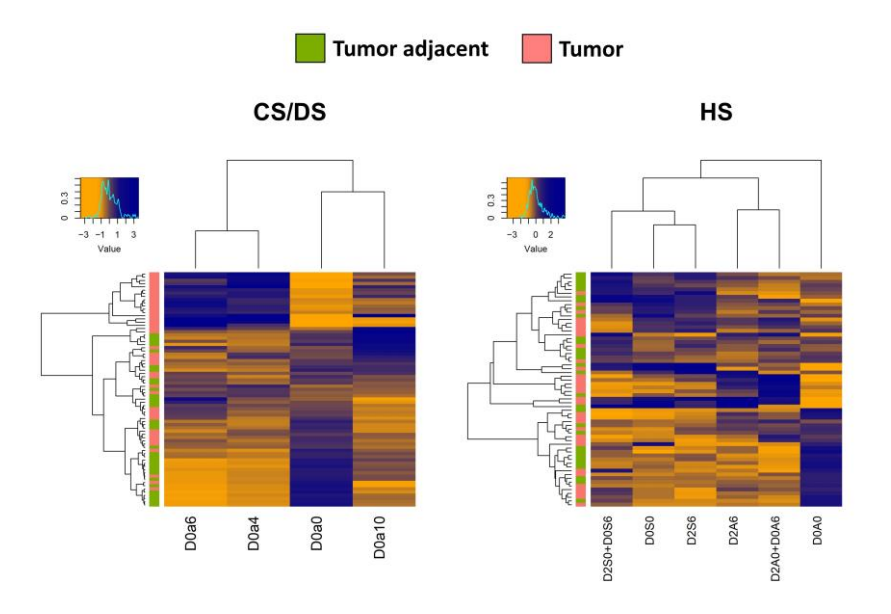


Figure 15. Hierarchical clustering of the CS/DS and HS disaccharides between all adjacent and all tumor samples represented by heatmap. The top left corner histogram shows correspondence between color hues and values.

4.2.2. CS/DS and HS content and sulfation characteristics between tumor and corresponding tumor adjacent normal samples

Performing comparison between tumor samples and their respective adjacent normal groups, significant changes were found in CS/DS sulfation level for the following disaccharides and derived values: D0a0, D0a4, and D0a6 disaccharides, total quantity of the CS/DS disaccharides, average degree of sulfation, and the 6-O/4-O-sulfation ratio (**Figure 16**). The abundance of D0a0 decreased, however the relative abundance of D0a4 and D0a6, and the average degree of sulfation, increased in all the examined lung tumor subtypes. The total CS/DS abundance showed an increased level for AC, SqCC, LCC. The 6-O/4-O-sulfation ratio decreased in the case of SCLC, SqCC, and LCC groups. The significant statistical results of CS/DS characteristics between the tumor and adjacent samples are shown in **Table 12**.

Comparisons between the tumor samples and their respective adjacent normal groups revealed no significant changes in HS sulfation levels and HS sulfation characteristics.

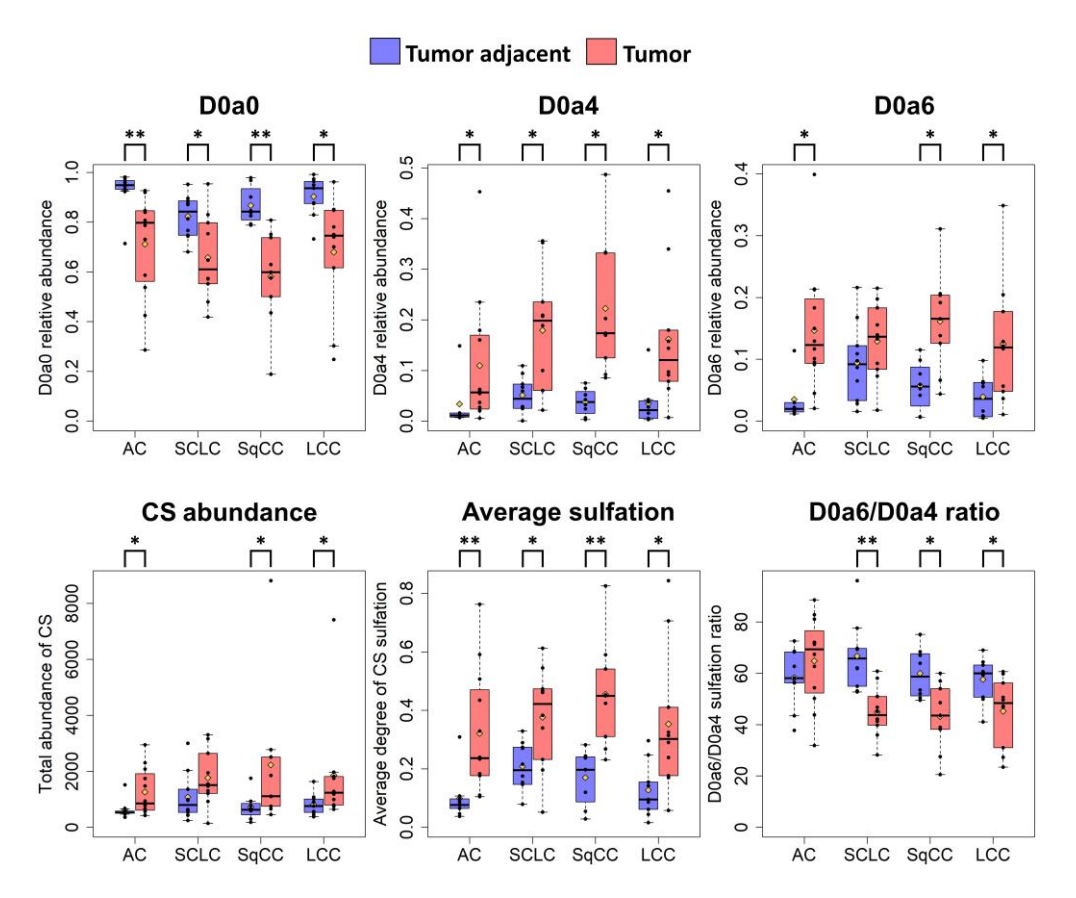


Figure 16. The differences in CS/DS sulfation patterns between the tumor and adjacent samples. Blue boxes indicate tumor-adjacent normal samples, while red boxes mark tumor samples. (AC: adenocarcinoma; SCLC: small cell lung cancer; SqCC: squamous cell carcinoma; LCC: large cell carcinoma). The yellow diamonds indicate the average values of the respective sample groups. (*: p < 0.05; **: p < 0.01).

Table 12. Summary of significant changes identified during the examination of CS/DS sulfation patterns between the tumor and adjacent samples.

Compared sample groups	Aspect of comparison	Tissue type	Number of tumor samples	Number of tumor adjacent samples	Statistical test	p-value	The degree of deviation (fold change)
		AC	12	9	Wilcoxon	<10-2	0.767
	D0-0	SCLC	10	10	Student t	< 0.05	0.799
	D0a0 quantity	SqCC	9	8	Student t	<10-2	0.669
		LCC	10	9	Student t	< 0.05	0.753
		AC	12	6	Welch t	< 0.05	3.241
	D0a4 quantity	SCLC	10	10	Welch t	< 0.05	3.513
		SqCC	9	8	Welch t	< 0.05	5.905
		LCC	10	8	Wilcoxon	< 0.05	4.625
	D0a6 quantity	AC	12	6	Wilcoxon	< 0.05	4.168
Tumor and		SqCC	9	8	Student t	< 0.05	2.820
respective		LCC	9	8	Student t	< 0.05	3.166
adjacent		AC	12	9	Wilcoxon	< 0.05	1.991
3	Total quantity	SqCC	9	8	Wilcoxon	< 0.05	3.068
		LCC	10	9	Wilcoxon	< 0.05	2.294
		AC	12	9	Wilcoxon	<10-2	3.238
	Average	SCLC	10	10	Student t	< 0.05	1.809
	sulfation	SqCC	9	8	Student t	<10-2	2.673
		LCC	10	9	Student t	< 0.05	2.779
	D0a6/D0a4-	SCLC	10	10	Student t	<10-2	0.673
		SqCC	9	8	Student t	< 0.05	0.719
	sulfation ratio	LCC	10	9	Student t	< 0.05	0.786

4.2.3. CS/DS and HS sulfation between lung tumor phenotypes

Comparing the different tumor phenotypes, the CS/DS 6-*O*/4-*O*-sulfation ratio showed a significant difference between the tumor groups. The 6-*O*/4-*O*-sulfation ratio of AC was significantly higher compared to all other tumor groups (**Figure 17**). No further significant differences between the tumor subtypes were identified either for the HS disaccharides considering the sulfation characteristics. The statistical results are in **Table 13**.

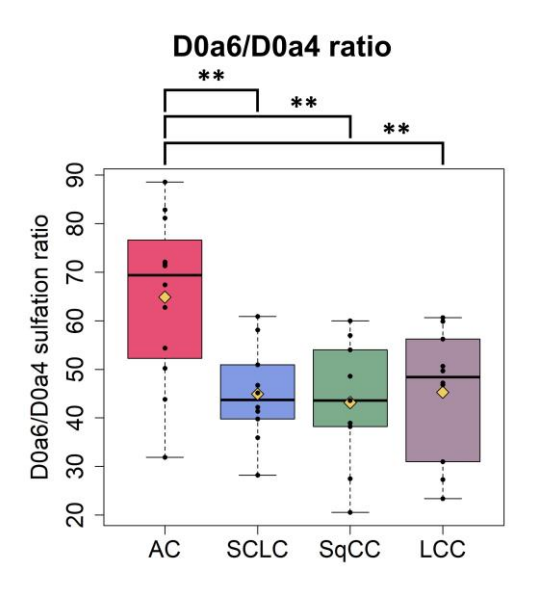


Figure 17. Distribution of CS/DS 6-O-/4-O-sulfation ratio between the investigated, different lung cancer subtypes (AC: adenocarcinoma, SCLC: small cell lung cancer, SqCC: squamous cell carcinoma, LCC: large cell carcinoma). The yellow diamonds indicate the average values of the respective sample groups. (**: p < 0.01).

Table 13. Summary of significant changes identified during the examination of CS/DS 6-*O*-/4-*O*-sulfation ratio between between the investigated, different lung cancer subtypes (AC: adenocarcinoma, SCLC: small cell lung cancer, SqCC: squamous cell carcinoma, LCC: large cell carcinoma).

Compared sample groups	Aspect of comparison	Tissue type	Number of tumor samples	Number of tumor adjacent samples	Statistical test	p-value	The degree of deviation (fold change)
	AC	AC	12	0			
Investigated	D0a6/D0a4-	SCLC	10	0	Student t	<10-2	1.443
tumor types	sulfation	SqCC	9	0	Student t	<10-2	1.503
**	ratio	LCC	10	0	Student t	<10-2	1.432

4.3. Analysis of lung adenocarcinoma sections with different genetic alterations

In this part of the study, the CS/DS GAG characteristics were investigated in AC tissue sections with different genetic alterations (ALK, EGFR, KRAS) and WT samples. The EGFR group could be further subdivided into the following subgroups according to the exact mutation type, which were the following: Exon 18, 19, 20 and 21 mutation. Totally, 96 samples were measured, including 8 ALK, 26 EGFR, 38 KRAS, 24 WT. The sample and patient details are summarized in **Table 6**. In some cases, a mismatch of the patients and clinical characteristics can be observed due to lack of data. Additionally, for the EGFR mutation type in three cases mutations in two different Exons were identified.

PCA was performed to consider the CS/DS disaccharides and their relative abundances (**Figure 18**). The analysis revealed no clear separation among the different genetic alterations. Additionally, other clinical factors, including sex, grade, stage, smoking and mutation type within the EGFR group, did not show any separation between the sample groups either.

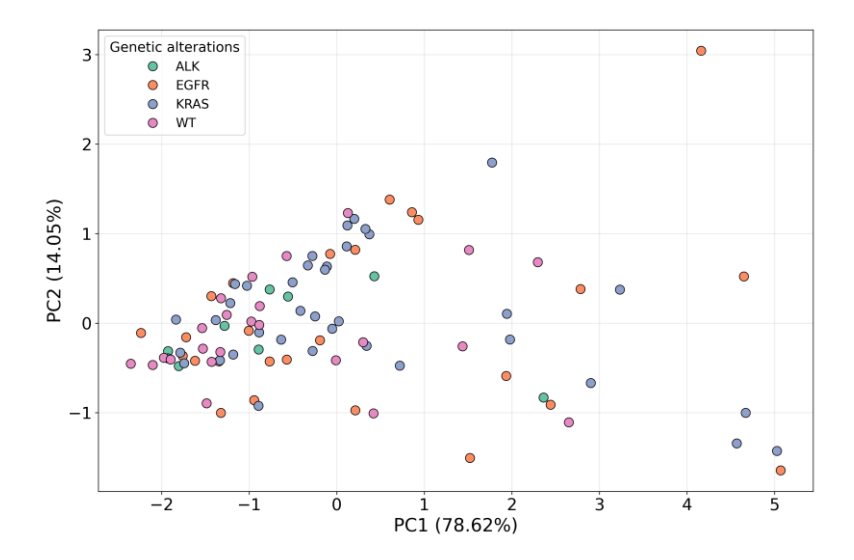


Figure 18. PCA of the CS/DS disaccharide relative abundances. The different colors indicate the different sample groups belonging to various genetic alterations (green for ALK, orange for EGFR, blue for KRAS and pink for WT).

4.3.1. CS/DS sulfation characteristics between the different genetic alterations

The sulfation characteristics of the sample groups were examined by comparing the relative abundances of D0a0, D0a4, D0a6 and D0a10 CS/DS disaccharides (calculated as their proportion of the total GAG disaccharide content) (**Figure 19**). Significantly higher relative abundance was observed for ALK and WT groups compared to EGFR group in the case of D0a4 disaccharide (**Figure 19**).

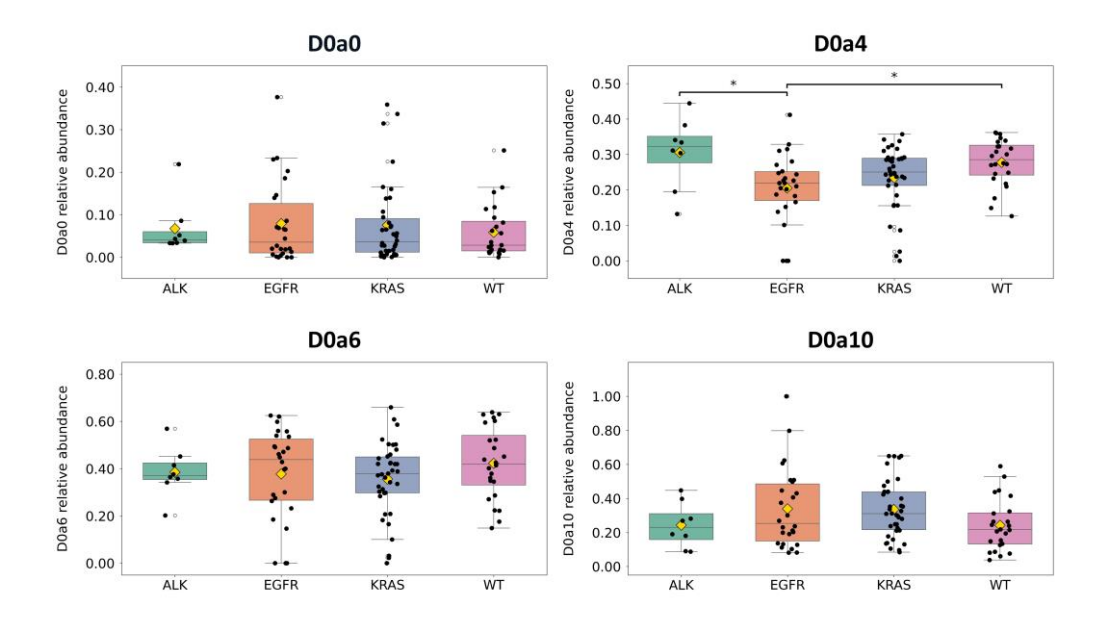


Figure 19. Box plots of CS/DS disaccharide relative abundances between the investigated sample groups. ALK: anaplastic lymphoma kinase, EGFR: epidermal growth factor receptor, KRAS: Kirsten rat sarcoma viral oncogene homolog, WT: wild type. The yellow diamonds indicate the average values of the respective sample groups.

6-O-/4-O-sulfation ratio and average degree of sulfation (**Figure 20**) were also investigated. 6-O-/4-O-sulfation ratio (Figure 20.) was significantly higher in the EGFR group compared to ALK sample group. The statistical results of the significantly different groups are summarized in **Table 14**.

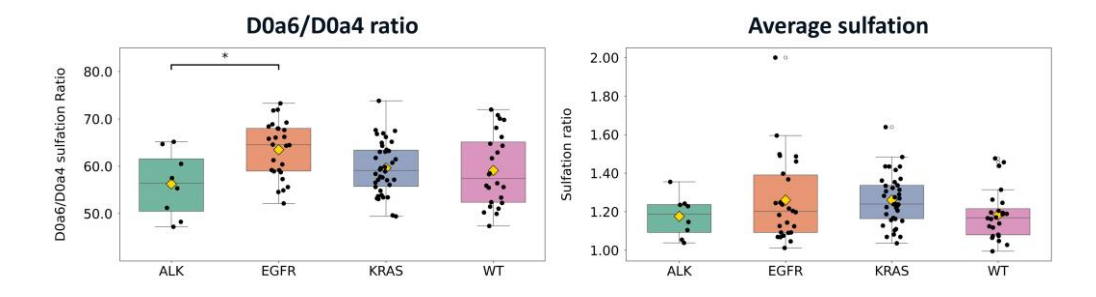


Figure 20. Box plots of CS/DS sulfation characteristics among the different genetic alterations. ALK: anaplastic lymphoma kinase, EGFR: epidermal growth factor receptor, KRAS: Kirsten rat sarcoma viral oncogene homolog, WT: wild type. The yellow diamonds indicate the average values of the respective sample groups.

Table 14. Summary of significant differences identified for CS/DS disaccharides between the investigated genetic alterations. (ALK: anaplastic lymphoma kinase, EGFR: epidermal growth factor receptor, WT: wild-type).

Way of comparison	Disaccharides	Disaccharides Significant pairs		Statistical test	Post hoc test	p-value	The degree of deviation (fold change)	
Relative concentration	D0a4	ALK – EGFR EGFR - WT	8 - 26 26 - 24	Kruskal- Wallis	Dunn	<0.05 <0.05	1.490 1.354	
ratio of CS/DS disaccharides between alterations	D0a6/D0a4	ALK - EGFR	8 - 26	ANOVA	Tukey HSD	<0.05	1.129	

As the EGFR sample group showed significant differences in the D0a4 relative abundance and 6-O-/4-O-sulfation ratio and detailed clinical information on specific EGFR mutation types were available, hierarchical clustering analysis was performed for CS/DS disaccharide relative abundances to examine patterns between the EGFR mutation types. No distinct clustering was observed according to the mutation types (**Figure 21**). While two main clusters are visible, by examining other parameters such as sex, grade, stage and smoking history we could not identify clustering in the case of EGFR samples either.

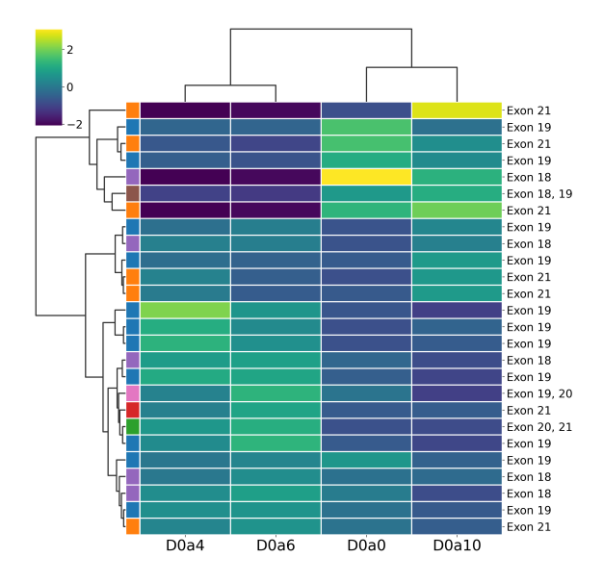


Figure 21. Hierarchical clustering of the CS/DS disaccharide relative abundances between the mutation types of the EGFR sample group represented by heatmap. The colors on the left represent the different genetic alterations, their names are shown on the right side.

5. Discussion

5.1. Stability studies of heparan sulfate

A common approach to study HS chains is to investigate their disaccharide building units. This type of analysis requires a lengthy sample preparation process, which can have a significant impact on the recovery and stability of the samples. However, these have not been systematically investigated in the literature before.

Since several steps require solvent exchange, it is important to investigate its impact on the samples. In line with our previous expectations, the most appropriate storage of biological samples is the dry frozen form. Furthermore, we observed molecular modifications occurring due to solvent evaporation (55 °C, over 1 h) in the case of Tris-HCl. We suggested that a covalent modification could have occurred between the HS disaccharides and Tris-HCl at elevated temperatures during extended periods of solvent evaporation (prolonged exposure to 55 °C). This result indicates a hydrophobic modification occurring on a specific subset of the molecules, leading to prolonged peak frontings. However, the modified product does not have high stability under the applied ESI conditions, and only the original HS disaccharide mass channels were observed. This hypothesis is supported by previous studies that have reported Tris-HCl forming imines with sterane compounds and carbohydrates at elevated temperature (116,117). In solution, the ring structure of sugars is in dynamic equilibrium with their linear forms. During this transformation, the sugar rings can open into chain forms, and the glycosidic hydroxyl group can be converted into an aldehyde oxo group, enabling imine formation. The products of this reaction could not be detected by MS, presumably due to the complete fragmentation in the ion source. As a result of this investigation, the use of AMBIC buffer is recommended for the digestion of HS chains to avoid the observed phenomenon.

Our results indicate that while liquid nitrogen freezing leads to greater sample loss, it also shows lower SD values. This provides more consistent results, which can be advantageous when analyzing biological samples.

The results are supported by the preliminary expectations that the stability of the HS disaccharides in aqueous solutions decreases with the increasing temperature. The conclusion drawn in the light of the results suggests that storage of samples in aqueous solution for 48 h at or below 4 °C, which temperature is commonly used in autosampler, is feasible, allowing the investigation of larger sample cohorts. In general, it is favorable

to choose the lowest possible temperature for sample storage to avoid sample degradation. However, in many cases, (e.g., during the sample preparation or before measurement in the autosampler) the temperature parameters are limited.

In correlation with our results, HS chains are known to remain stable under neutral pH conditions for longer time periods. Our observations emphasize the importance of selecting the optimal pH for preserving HS disaccharide samples. It has been proven that storing samples under neutral conditions is the most favorable, allowing preservation for up to 24 h. While acidic pH is also suitable for most disaccharides, it is not ideal for long-term storage. Basic conditions should be avoided due to significant sample degradation, consistent with previous literature reporting HS chains degradation under basic conditions (118).

Considering the storage vessels, based on the results, plastic tubes are the preferred option for sample storage, especially when the samples are stored in water, as this helps reduce the rate of sample precipitation. This can be explained by the fact that HS disaccharides are significantly more soluble in water.

Based on our statistical results, the 10 mM ammonium formate in 75:25% ACN:water mixture (solvent d) provided the most reliable results as injection solvent for all the investigated disaccharides. This aligns with the previous observations on CS disaccharides (73).

In this study, various sample preparation steps and storage parameters were examined which are required in the GAG analysis of biological samples through their disaccharide building units. The parameters that were considered as optimal are listed in **Table 9**.

5.2. Analysis of lung tumor sections with different cancer subtypes

Based on the current knowledge, no prior study has undertaken a direct comparison of the CS/DS and HS GAG sulfation characteristics in FFPE tissues of SCLC and various NSCLC subtypes, including AC, SqCC and LCC and their respective tumor adjacent normal regions. Examining the differences between all the tumor and all the adjacent samples, several significant differences were identified in the total CS/DS disaccharide abundance and in the relative quantity of non-sulfated (D0a0) and mono-sulfated (D0a4 and D0a6) disaccharides. We observed differences in the mono-*O*-sulfated (D2A0 + D0A6) and di-sulfated (1-*O*- and 1-*N*-sulfated) (D2S0 + D0S6) HS between the tumor and tumor adjacent samples. In the case of CS/DS, we found significant differences in the

average degree of sulfation and the 6-O-/4-O-sulfation ratio between the tumor and tumor adjacent normal samples consistently across most of the group comparisons. We also recognized alterations in the mono-, di-, and total-N/O-sulfation levels of HS between the tumor and tumor adjacent samples. Investigating the sulfation characteristics of CS/DS between the tumorous groups and their corresponding adjacent normal samples, we identified changes in the level of non-sulfated (D0a0) and the mono-sulfated (D0a4) disaccharides and the overall degree of sulfation also changed in all tumor sample groups. The 6-O-/4-O-sulfation ratio of CS/DS disaccharides differentiated AC from all the other lung tumor subtypes investigated. In the literature, several articles highlight the changes and correlation of 6-O- and 4-O-sulfated CS disaccharides with various diseases like osteoarthritis and rheumatoid arthritis (119), neurological disorders (120), cardiovascular disease (121), metabolic disorders (122) and in various cancers such as ovarian cancer (123). The changes of the CS disaccharides are not only markers of the diseases but may also play a dominant role in the disease progression through cellular interactions. In some cases, elevated level of 4-O-sulfation have been associated with pro-inflammatory (124) and pro-tumorigenic environment (125). In contrast, 6-O-sulfation might have a more protective role in certain tissues (126). Research suggests that the sulfation ratio of 4-Oand 6-O-sulfation may play an important role in the interaction between the tumor and tumor-adjacent regions, potentially affecting the tumor development and spread. Oncofetal chondroitin sulfate (ofCS) is a specific glycosaminoglycan modification that is typically found in the placenta tissue during fetal development. Of CS is re-expressed and predominantly characterized with high degree of 4-O-sulfation and low 6-O-/4-Osulfation ratio on N-acetylgalactosamine residues in several cancers including colorectal and lung cancer (127). This pattern matches the findings of increased 4-sulfated to 6sulfated CS disaccharide ratios in tumor tissues detected in our analysis, suggesting it may contribute to tumor growth and metastasis (128). In addition to increased 4-Osulfation, the presence of of CS can be detected through its specific binding to the recombinant VAR2CSA malaria protein (128). In tumor and placental tissue dodecasaccharide (dp12) was identified as the minimal length of the CS-binding domain of the malarial VAR2CSA protein. This domain contains mostly 4-O-sulfated and some 6-O-sulfated N-acetylgalactosamine residues (128). In our investigation, we observed a significant increase in the abundance of D0a4 (AC, SCLC, SqCC, and LCC) and D0a6

(AC, SqCC, and LCC) sulfated CS disaccharides in the tumor tissue samples. The decrease of 6-O-/4-O-sulfation ratio was also observed between the tumor samples with exception of AC. Furthermore, in a recent study of lung cancer, elevated of CS level has been associated with poor disease-free and overall survival in early-stage NSCLC, regardless of presence of KRAS and EGFR mutations (127). These observations may suggest the possible presence of ofCS in our analyzed sample cohort. The discussed results suggest the importance of further investigation of CS disaccharides in different lung tumor phenotypes. For a small number of samples (3 AC, 3 SqCC, and 5 control), the comparison of the total GAG content and specific GAG classes have already performed in lung carcinoma samples and distant normal tissues (90). In a quantitative GAG study the changes in the GAG abundances were also observed in different LC subtypes (2 SqCC, 4 AC, and 5 SCLC) (91). In these initial studies the GAG content of the tissues were investigated through classical methods such as cellulose acetate electrophoresis as well as chemical and enzymatic digestions. In our presented investigation the total CS/DS content in all the LC types investigated compared to the adjacent samples also showed an increased level in line with the literature. The comprehensive investigation of GAG composition in relation with the subtype and degree of differentiation status of lung carcinomas was conducted through the analysis of 34 samples using histochemistry and spectrophotometry (129). It has been shown that the total GAG content was found to be higher in lung cancer phenotypes compared to normal lung tissue. Additionally, significant differences were also observed in the GAG fractions compared with poorly differentiated and nonciliated bronchiolar cell type (Clara cell type) adenocarcinomas (129). Previously, the different types of lung cancer were not considered in detail in disaccharide-specific analysis. The most comprehensive results were reported by Li et al. in a study involving small sample cohort of SqCC (92). To compare the structure of GAGs, glycolipids, and selected proteins the authors investigated 10 SqCC and corresponding patient-matched normal tissues by using liquid chromatography and Western blotting techniques. Although their investigation was limited to SqCC tissues, most of their results correlate with our results. Li et al. identified that the total HS content was not different between SqCC and normal tissue, while the CS/DS content was two times higher in the case of SqCC. All of the mentioned studies were also in correlation with our presented results. Furthermore, we could identify

significant difference only in CS/DS content between the investigated tumor and adjacent tissue samples, but not in the case of HS quantity. Li et al. observed for HS disaccharides that, the tri-sulfated (D2S6), mono-N-sulfated (D0S0), and non-sulfated (D0A0) disaccharides were not different between normal and SqCC tissues, while the amount of di- (D0S6, D2S0), and mono-O-sulfated (D2A0) disaccharides showed lower abundance in tumor samples. In line with these observations, our results also show that the amount of tri- (D2S6), mono-N-sulfated (D0S0), and non-sulfated (D0A0) disaccharides did not change in the tumor tissues compared to adjacent regions. Furthermore, the decrease in the di-sulfated (D2S0, D0S6) disaccharides was also observed, but in contrast, the monosulfated (D2A0, D0A6) disaccharides showed a significantly increased quantity in the tumor samples. For CS/DS disaccharides, Li et al. identified the changes in the quantity of mono-sulfated disaccharides. The level of D0a4 decreased, while D0a6 increased in SqCC tissues, while in our study both D0a4 and D0a6 increased in different tumor types compared to the respective tumor adjacent tissue. Moreover, we also observed a decrease in the case of the non-sulfated (D0a0) component for all examined tumor tissue types compared to their adjacent tissue. These divergent observations establish a basis for future, larger-scale studies and validation of results through complementary techniques. Our research group also identified several significant differences in the protein profiles of the various LC types (SCLC, AC, SqCC, and LCC) through shotgun proteomics on the same sample cohort as investigated in this study (130). The identified proteoglycan core proteins included versican, which was overexpressed in AC, while perlecan, decorin, prolargin, and mimecan were underexpressed in SCLC and LCC. Additionally, biglycan was underexpressed in AC, SCLC, and SqCC (130,131). Versican and biglycan are CS proteoglycans (132,133). The increased expression of versican was identified in AC, consistent with our current observation of increased total CS/DS GAG abundance. Furthermore, versican is among the chondroitin sulfate proteoglycan (CSPG) core proteins that carry VAR2CSA-binding oncofetal CS (134).

Additionally, a previous study demonstrated that the proteoglycan serglycin (SRGN) was shown to promote NSCLC cell migration (135). NSCLC cells express SRGN, a highly glycosylated protein that is predominantly composed of CS/DS- and fewer HS-GAG chains. The CS component of SRGN facilitates binding to CD44 on the surface of tumor

cells, supporting cell migration. This interaction does not occur in the absence of CS chains (135).

Based on previous observations, CS plays an important biological role in tumor microenvironment formation. CS has been implicated in mediating interactions between cell-cell and cell-ECM in solid tumors, thereby leading to aggressive spread and metastasis of tumor by promoting tumor cell adhesion and migration (136). Our findings have revealed several significant differences in CS associated with lung cancer. Elevated CS abundance has been already observed in various tumor types, e.g., liver, prostate demonstrating the importance of CS in tumor formation (88,89). In our investigation, the quantity of CS increased in tumor samples, suggesting increased activity of enzymes responsible for CS biosynthesis.

5.3. Analysis of lung tumor sections with different genetic alterations

To our knowledge, this study is the first to examine CS/DS GAGs in the case of different genetic alterations in lung AC samples. GAGs and PGs through their interactions with receptor tyrosine kinases (RTKs) are integral to tumor progression (11). GAGs have been studied in the context of their binding and activation with ALK and EGFR proteins, which are RTKs. The clustering and activation of the receptors are affected by the variable sulfation of the disaccharide building blocks of GAGs. An example of the mentioned relationship, decorin a CS/DS proteoglycan inhibits multiple RTK signaling pathways in various cancer types by upregulating p21, a crucial cell cycle regulator (11). HSPGs are in interaction with HS-binding proteins in the extracellular matrix and on the cell surface, thereby modulating various biological activities. Their involvement in growth factorreceptor interactions and RTK activation highlights their potential as therapeutic targets to disrupt oncogenic signaling in tumors (137). CS/DS PGs are primarily located in the extracellular matrix of tumors, but they are also present on the membranes of cancer cells, including CD44 and CSPG4 PGs. Our research group identified CS/DS chains carrying core proteins by MS-based proteomics, including versican, biglycan, and CD44 in all the samples investigated in cohort of the present study. Furthermore, decorin and CSPG4 were present in most of the samples investigated (138). Biglycan has previously been proposed as a LC biomarker (11,139). These observations highlight the necessity of investigating the structure characteristics of CS/DS chains in CSPGs within LC samples.

This analysis can be performed using MS or antibodies recognizing specific epitopes, such as of CS.

Clausen et al. proved that of CS has a crucial role in regulating cancer cell migration and metastasis regulation through integrin signaling pathways (140). Of CS, typically confined to placental tissue, is aberrantly overexpressed in various solid tumors, including melanoma and muscle-invasive bladder cancer in correlation with advanced tumor stages and poor patient prognosis (140-142). Zarni Oo et al. attempted to examine of CS expression in NSCLC and its potential as a therapeutic target (90). Their results demonstrated that elevated of CS expression is associated with reduced disease-free survival and overall survival, with higher of CS levels in EGFR/KRAS wild-type cases compared to mutated samples (127), in correlation with that, our observations also indicate an increased abundance of the 4-O-sulfated D0a4 disaccharide in WT samples compared to ALK, EGFR, and KRAS groups. This distinct expression pattern of of CS makes them potential for targeted cancer therapies. Machino et al. showed that DS directly binds to the extracellular N-terminal region of ALK, triggering its activation (143). Comparable interactions have been observed with HS and its over sulfated form, heparin (144). Using the human neuroblastoma cell line (NB-1), known for its high expression of wild-type ALK, they discovered that the DS tetrasaccharide alone was enough to trigger ALK autophosphorylation at tyrosine 1604, a key indicator of its activation (143). Longer oligosaccharides enhanced ALK activation, resembling the pattern seen with HS. Additionally, Murray et al. showed that HS modulates ALK activation based on its length, with octasaccharide HS binding to ALK's N-terminal basic amino acid cluster, while longer HS chains facilitate receptor clustering and activation (145). These findings highlight the critical role of glycans as signaling molecules in ALK activation and their impact on tumor pathophysiology.

We performed PCA of CS/DS disaccharides for their relative abundances, but no distinct separation was revealed between the investigated sample groups. However, significant differences were identified in the relative abundance of the D0a4 disaccharide and in the 6-O-/4-O-sulfation ratio between EGFR and WT groups. Furthermore, the EGFR and ALK groups exhibited significant differences in the relative abundance of D0a4 disaccharide. Both EGFR and ALK are RTKs, differences in CS/DS sulfation patterns may affect their binding affinities and interactions. The analysis of CS/DS disaccharide

abundance in the EGFR mutated sample group showed no distinct clustering among different EGFR mutation subtypes. This observation was particularly relevant, as EGFR mutation status plays a critical role in determining the effectiveness of tyrosine kinase inhibitor therapies (144). In our study, most samples with EGFR mutation exhibited either exon 19 deletions or mutations in exons 18 and 21, which are associated with increased sensitivity to EGFR tyrosine kinase inhibitors. Previous studies have reported that ALK, EGFR and KRAS genetic alterations affect the prognosis and treatment response in AC. The differences in CS/DS disaccharide profiles observed in AC samples with various genetic alterations in this work suggest that GAG modifications could be valuable biomarkers for diagnostic or prognostic purposes. These observations emphasize the need for further studies to deeper understand the role of GAGs in the mechanism of lung cancer.

6. Conclusions

6.1. Stability studies of heparan sulfate

Several parameters were identified, which affect the stability and recovery of HS disaccharides during the sample preparation process.

- a) Evaporation of HS disaccharide samples from Tris-HCl containing solvent in heated vacuum centrifuge should be avoided.
- b) Storage of HS disaccharide samples under alkaline conditions is not recommended.
- c) It is advisable to avoid frequent thawing and freezing of HS disaccharide samples, however if it is necessary rapid freezing is preferred using liquid nitrogen (-196 °C).
- d) The storage of HS disaccharides is safe under neutral pH conditions for up to 24 h at room temperature and even up to 48 h at 4 °C.
- e) Ammonium formate salt additive enhances the stability of the multiply sulfated HS disaccharides in both ACN and MeOH-based solvents.
- f) HS disaccharide precipitation can be reduced by using aqueous solution and storage in plastic tubes.

6.2. Analysis of lung tumor sections with different cancer subtypes

CS/DS and HS disaccharide content and sulfation of various lung tumor phenotypes and corresponding adjacent normal tissues were analyzed. Significant differences in the quantity and sulfation of CS/DS and HS GAGs were identified.

- a) The total abundance of CS/DS disaccharides was doubled in tumor samples.
- b) The total abundance of HS disaccharides did not change significantly.
- c) The average degree of CS/DS sulfation significantly increased in all the investigated tumor phenotypes compared to the adjacent normal tissue.
- d) The CS 6-O-/4-O-sulfation ratio was elevated in AC compared to the other lung tumor phenotypes investigated.
- e) O-sulfated HS components increased in tumor samples.

6.3. Analysis of lung adenocarcinoma sections with different genetic alterations

CS/DS GAGs characteristics were investigated in case of genetic alterations in ALK, EGFR and KRAS oncogenes and wild-type lung AC tissue. The different genetic alterations showed a high similarity in CS/DS abundance and sulfation characteristics, but in some cases, significant differences were observed between the sample groups.

- a) The D0a4 relative abundance for the ALK and EGFR groups was significantly different compared to the WT sample group.
- b) In the case of 6-O-/4-O-sulfation ratio the ALK and EGFR sample groups were found to be significantly different from each other.

7. Summary

Over the course of my doctoral work, the following three research projects were conducted: investigation of sample handling steps for accurate HS disaccharide analysis using HPLC-MS; compositional analysis of CS/DS and HS glycosaminoglycans in different lung cancer phenotypes; analysis and characterization of CS/DS composition of lung adenocarcinoma tissues with different types of genetic alterations in ALK, EGFR and KRAS oncogenes.

In the stability studies, we aimed to investigate the parameters involved in GAG sample preparation, including the drying and storage of samples under different conditions, to significantly increase the efficiency of the analytical measurements of HS GAGs. We have identified the limitations of HS disaccharide storage, including temperature, time, repeated thawing and freezing and the effects of drying. We also investigated the most suitable buffer for the digestion of HS chains.

In the second research project, our aim was to investigate and compare the composition of CS/DS and HS GAGs in different lung tumor subtypes and the surrounding normal tissue. We identified several differences in the abundance and sulfation characteristics of CS/DS disaccharides, however for HS disaccharides only a few significant changes were observed between the tumor and tumor adjacent tissues. Comparing the tumor groups, no significant differences were observed, except in the 6-*O*-/4-*O*-sulfation ratio in the case of CS/DS disaccharides, where the AC sample group showed difference from the other lung cancer phenotypes.

Since several significant differences were observed for the CS/DS GAG class, we further investigated the relationships between CS/DS disaccharides and lung cancer. We performed the analysis and characterization of CS/DS composition of lung adenocarcinoma tissues with different type of genetic alterations in ALK, EGFR and KRAS oncogenes. The different genetic alterations showed similarities, but in some cases, we could identify significant differences between ALK and EGFR sample groups, including D0a4 disaccharide abundance and 6-*O*-/4-*O*-sulfation ratio. These observations support the association of CS/DS GAGs with different genetic alterations in AC.

8. References

- 1. Lin H, Begley T. Protein posttranslational modifications: chemistry, biology, and applications. Mol Biosyst. 2011;7(1):14–5.
- 2. Zhong Q, Xiao X, Qiu Y, Xu Z, Chen C, Chong B, et al. Protein posttranslational modifications in health and diseases: Functions, regulatory mechanisms, and therapeutic implications. MedComm. 20231;4(3):e261.
- 3. Esko JD, Kimata K, Lindahl U. Proteoglycans and sulfated glycosaminoglycans. Essentials Glycobiol 2nd Ed. 2009;
- Lemjabbar-Alaoui H, McKinney A, Yang Y-W, Tran VM, Phillips JJ. Chapter Nine - Glycosylation Alterations in Lung and Brain Cancer. In: Drake RR, Ball LEBT-A in CR, editors. Glycosylation and Cancer. Academic Press; 2015. p. 305– 44.
- 5. Spiro RG. Glycoproteins. In: Anfinsen CB, Edsall JT, Richards FMBT-A in PC, editors. Academic Press; 1973. p. 349–467.
- 6. Couchman JR, Pataki CA. An Introduction to Proteoglycans and Their Localization. J Histochem Cytochem. 2012;60(12):885–97.
- 7. Gibbs R V. Cytokines and Glycosaminoglycans (GAGS) BT Glycobiology and Medicine. In: Axford JS, editor. Boston, MA: Springer US; 2003. p. 125–43.
- 8. Kjellén L, Lindahl U. Specificity of glycosaminoglycan–protein interactions. Curr Opin Struct Biol. 2018;50:101–8.
- 9. Kreuger J, Kjellén L. Heparan Sulfate Biosynthesis: Regulation and Variability. J Histochem Cytochem. 2012;60(12):898–907.
- Mizumoto S, Yamada S. The Specific Role of Dermatan Sulfate as an Instructive Glycosaminoglycan in Tissue Development. Vol. 23, International Journal of Molecular Sciences. 2022.
- 11. Ricard-Blum S, Vivès RR, Schaefer L, Götte M, Merline R, Passi A, et al. A biological guide to glycosaminoglycans: current perspectives and pending questions. FEBS J. 2024;291(15):3331–66.

- 12. Mizumoto S, Yamada S. An Overview of in vivo Functions of Chondroitin Sulfate and Dermatan Sulfate Revealed by Their Deficient Mice. Front Cell Dev Biol. 2021;9.
- 13. Parker JL, Newstead S. Gateway to the Golgi: molecular mechanisms of nucleotide sugar transporters. Curr Opin Struct Biol. 2019;57:127–34.
- Zimmer Brenna M, Barycki Joseph J, Simpson Melanie A. Integration of Sugar Metabolism and Proteoglycan Synthesis by UDP-glucose Dehydrogenase. J Histochem Cytochem. 2020;69(1):13–23.
- 15. Izumikawa T, Koike T, Shiozawa S, Sugahara K, Tamura J, Kitagawa H. Identification of Chondroitin Sulfate Glucuronyltransferase as Chondroitin Synthase-3 Involved in Chondroitin Polymerization: CHONDROITIN POLYMERIZATION IS ACHIEVED BY MULTIPLE ENZYME COMPLEXES CONSISTING OF CHONDROITIN SYNTHASE FAMILY MEMBERS. J Biol Chem. 2008;283(17):11396–406.
- 16. Mizumoto S, Yamada S. Histories of Dermatan Sulfate Epimerase and Dermatan 4-O-Sulfotransferase from Discovery of Their Enzymes and Genes to Musculocontractural Ehlers-Danlos Syndrome. Vol. 14, Genes. 2023;14(2): 509.
- 17. Pagielska M, Samsonov SA. Molecular Dynamics-Based Comparative Analysis of Chondroitin and Dermatan Sulfates. Vol. 13, Biomolecules. 2023;13(2), 247.
- Syx D, Delbaere S, Bui C, De Clercq A, Larson G, Mizumoto S, et al. Alterations in glycosaminoglycan biosynthesis associated with the Ehlers-Danlos syndromes.
 Am J Physiol Physiol. 2022;323(6):C1843–59.
- 19. Li J-P, Kusche-Gullberg M. Chapter Six Heparan Sulfate: Biosynthesis, Structure, and Function. In: Jeon KWBT-IR of C and MB, editor. International Review of Cell and Molecular Biology. Academic Press; 2016; 325:215-273.
- 20. Annaval T, Wild R, Crétinon Y, Sadir R, Vivès RR, Lortat-Jacob H. Heparan Sulfate Proteoglycans Biosynthesis and Post Synthesis Mechanisms Combine Few Enzymes and Few Core Proteins to Generate Extensive Structural and Functional Diversity. Vol. 25, Molecules. 2020; 25(18):4215.

- 21. Presto J, Thuveson M, Carlsson P, Busse M, Wilén M, Eriksson I, et al. Heparan sulfate biosynthesis enzymes EXT1 and EXT2 affect NDST1 expression and heparan sulfate sulfation. Proc Natl Acad Sci. 2008;105(12):4751–6.
- 22. Sanderson RD, Yang Y, Suva LJ, Kelly T. Heparan sulfate proteoglycans and heparanase—partners in osteolytic tumor growth and metastasis. Matrix Biol. 2004;23(6):341–52.
- 23. Toole BP. Hyaluronan: from extracellular glue to pericellular cue. Nat Rev Cancer. 2004;4(7):528–39.
- 24. Sasisekharan R, Shriver Z, Venkataraman G, Narayanasami U. Roles of heparansulphate glycosaminoglycans in cancer. Nat Rev Cancer. 2002;2(7):521–8.
- 25. Filmus J. Glypicans in growth control and cancer. Glycobiology. 2001;11(3):19R-23R.
- Morla S. Glycosaminoglycans and Glycosaminoglycan Mimetics in Cancer and Inflammation. Vol. 20, International Journal of Molecular Sciences. 2019; 20(8): 1963.
- 27. Bernfield M, Götte M, Park PW, Reizes O, Fitzgerald ML, Lincecum J, et al. Functions of cell surface heparan sulfate proteoglycans. Annu Rev Biochem. 1999;68(1):729–77.
- 28. Afratis N, Gialeli C, Nikitovic D, Tsegenidis T, Karousou E, Theocharis AD, et al. Glycosaminoglycans: key players in cancer cell biology and treatment. FEBS J. 2012;279.
- 29. Ho W-L, Hsu W-M, Huang M-C, Kadomatsu K, Nakagawara A. Protein glycosylation in cancers and its potential therapeutic applications in neuroblastoma. J Hematol Oncol. 2016;9(1):100.
- 30. Wuyts W, Van Hul W. Molecular basis of multiple exostoses: mutations in the EXT1 and EXT2 genes. Hum Mutat. 2000;15(3):220–7.
- 31. Jayson GC, Lyon M, Paraskeva C, Turnbull JE, Deakin JA, Gallagher JT. Heparan Sulfate Undergoes Specific Structural Changes during the Progression from

- Human Colon Adenoma to Carcinoma in vitro. J Biol Chem. 1998;273(1):51–7.
- 32. Raman K, Kuberan B. Chemical tumor biology of heparan sulfate proteoglycans. Curr Chem Biol. 2010;4(1):20–31.
- 33. Marolla APC, Waisberg J, Saba GT, Waisberg DR, Margeotto FB, Pinhal MA da S. Glycomics expression analysis of sulfated glycosaminoglycans of human colorectal cancer tissues and non-neoplastic mucosa by electrospray ionization mass spectrometry. Einstein (Sao Paulo). 2015;13(4):510–7.
- 34. Esko JD, Selleck SB. Order out of chaos: assembly of ligand binding sites in heparan sulfate. Annu Rev Biochem. 2002;71(1):435–71.
- 35. Nikitovic D, Chatzinikolaou G, Tsiaoussis J, Tsatsakis A, Karamanos NK, Tzanakakis GN. Insights into Targeting Colon Cancer Cell Fate at the Level of Proteoglycans / Glycosaminoglycans. Current Medicinal Chemistry. 2012;19(25): 4247-4258.
- 36. Porcionatto MA, Nader HB, Dietrich CP. Heparan sulfate and cell division. Brazilian J Med Biol Res. 1999;32:539–44.
- 37. Izumikawa T, Kanagawa N, Watamoto Y, Okada M, Saeki M, Sakano M, et al. Impairment of Embryonic Cell Division and Glycosaminoglycan Biosynthesis in Glucuronyltransferase-I-deficient Mice. J Biol Chem. 2010;285(16):12190–6.
- 38. Fernández-Vega I, García-Suárez O, García B, Crespo A, Astudillo A, Quirós LM. Heparan sulfate proteoglycans undergo differential expression alterations in right sided colorectal cancer, depending on their metastatic character. BMC Cancer. 2015;15(1):742.
- 39. Theocharis AD, Skandalis SS, Tzanakakis GN, Karamanos NK. Proteoglycans in health and disease: novel roles for proteoglycans in malignancy and their pharmacological targeting. FEBS J. 2010;277(19):3904–23.
- 40. Moon S, Zhao Y-T. Spatial, temporal and cell-type-specific expression profiles of genes encoding heparan sulfate biosynthesis enzymes and proteoglycan core proteins. Glycobiology. 2021;31(10):1308–18.

- 41. Reed CC, Waterhouse A, Kirby S, Kay P, Owens RT, McQuillan DJ, et al. Decorin prevents metastatic spreading of breast cancer. Oncogene. 2005;24(6):1104–10.
- 42. Köninger J, Giese NA, di Mola FF, Berberat P, Giese T, Esposito I, et al. Overexpressed Decorin in Pancreatic Cancer: Potential Tumor Growth Inhibition and Attenuation of Chemotherapeutic Action. Clin Cancer Res. 2004;10(14):4776–83.
- 43. Tralhão JG, Schaefer L, Micegova M, Evaristo C, Schönherr E, Kayal S, et al. In vivo selective and distant killing of cancer cells using adenovirus-mediated decorin gene transfer. FASEB J Off Publ Fed Am Soc Exp Biol. 2003;17(3):464–6.
- 44. Ahrens TD, Bang-Christensen SR, Jørgensen AM, Løppke C, Spliid CB, Sand NT, et al. The Role of Proteoglycans in Cancer Metastasis and Circulating Tumor Cell Analysis. Front Cell Dev Biol. 2010; 285(16): 12190-12196.
- 45. Suhovskih A V, Mostovich LA, Kunin IS, Boboev MM, Nepomnyashchikh GI, Aidagulova S V, et al. Proteoglycan Expression in Normal Human Prostate Tissue and Prostate Cancer. Int Sch Res Not. 2013;2013(1):680136.
- 46. True LD, Hawley S, Norwood TH, Braun KR, Evanko SP, Chan CK, et al. The accumulation of versican in the nodules of benign prostatic hyperplasia. Prostate. 2009;69(2):149–58.
- 47. Henke A, Grace OC, Ashley GR, Stewart GD, Riddick ACP, Yeun H, et al. Stromal Expression of Decorin, Semaphorin6D, SPARC, Sprouty1 and Tsukushi in Developing Prostate and Decreased Levels of Decorin in Prostate Cancer. PLoS One. 2012;7(8):e42516.
- 48. Luo J, Dunn T, Ewing C, Sauvageot J, Chen Y, Trent J, et al. Gene expression signature of benign prostatic hyperplasia revealed by cDNA microarray analysis. Prostate. 2002;51(3):189–200.
- 49. Shimada K, Nakamura M, De Velasco MA, Tanaka M, Ouji Y, Konishi N. Syndecan-1, a new target molecule involved in progression of androgen-independent prostate cancer. Cancer Sci. 2009;100(7):1248–54.

- 50. Inki P, Jalkanen M. The Role of Syndecan-1 in Malignancies. Ann Med. 1996;28(1):63–7.
- 51. Quach ND, Kaur SP, Eggert MW, Ingram L, Ghosh D, Sheth S, et al. Paradoxical Role of Glypican-1 in Prostate Cancer Cell and Tumor Growth. Sci Rep. 2019;9(1):11478.
- 52. WIKSTEN J-P, LUNDIN J, NORDLING S, KOKKOLA A, HAGLUND CAJ. Comparison of the Prognostic Value of a Panel of Tissue Tumor Markers and Established Clinicopathological Factors in Patients with Gastric Cancer. Anticancer Res. 2008;28(4C):2279 LP 2287.
- 53. Wei J, Hu M, Huang K, Lin S, Du H. Roles of Proteoglycans and Glycosaminoglycans in Cancer Development and Progression. Vol. 21, International Journal of Molecular Sciences. 2020; 21(17): 5983.
- 54. Perez S, Makshakova O, Angulo J, Bedini E, Bisio A, de Paz JL, et al. Glycosaminoglycans: What Remains To Be Deciphered? JACS Au. 2023;3(3):628–56.
- 55. Wang Z, Zhang F, S Dordick J, J Linhardt R. Molecular mass characterization of glycosaminoglycans with different degrees of sulfation in bioengineered heparin process by size exclusion chromatography. Curr Anal Chem. 2012;8(4):506–11.
- 56. Solakyildirim K. Recent advances in glycosaminoglycan analysis by various mass spectrometry techniques. Anal Bioanal Chem. 2019;411(17):3731–41.
- 57. ten Dam GB, van de Westerlo EMA, Purushothaman A, Stan R V, Bulten J, Sweep FCGJ, et al. Antibody GD3G7 Selected against Embryonic Glycosaminoglycans Defines Chondroitin Sulfate-E Domains Highly Up-Regulated in Ovarian Cancer and Involved in Vascular Endothelial Growth Factor Binding. Am J Pathol. 2007;171(4):1324–33.
- 58. Lawrence R, Lu H, Rosenberg RD, Esko JD, Zhang L. Disaccharide structure code for the easy representation of constituent oligosaccharides from glycosaminoglycans. Nat Methods. 2008;5(4):291–2.
- 59. Zhang T, Zhang R, Lv Y, Wang M, Li H, Tan T, et al. Glycosaminoglycans in

- biological samples Towards identification of novel biomarkers. TrAC Trends Anal Chem. 2020;122:115732.
- 60. Shao C, Shi X, Phillips JJ, Zaia J. Mass Spectral Profiling of Glycosaminoglycans from Histological Tissue Surfaces. Anal Chem. 2013;85(22):10984–91.
- 61. Dong X, Huang Y, Cho BG, Zhong J, Gautam S, Peng W, et al. Advances in mass spectrometry-based glycomics. Electrophoresis. 2018;39(24):3063–81.
- 62. Turiák L, Tóth G, Ozohanics O, Révész Á, Ács A, Vékey K, et al. Sensitive method for glycosaminoglycan analysis of tissue sections. J Chromatogr A. 2018;1544:41–8.
- 63. Lv H, Yu G, Sun L, Zhang Z, Zhao X, Chai W. Elevate Level of Glycosaminoglycans and Altered Sulfation Pattern of Chondroitin Sulfate Are Associated with Differentiation Status and Histological Type of Human Primary Hepatic Carcinoma. Oncology. 2008;72(5–6):347–56.
- 64. Suzuki S, Saito H, Yamagata T, Anno K, Seno N, Kawai Y, et al. Formation of Three Types of Disulfated Disaccharides from Chondroitin Sulfates by Chondroitinase Digestion. J Biol Chem. 1968;243(7):1543–50.
- 65. Laremore TN, Leach FE 3rd, Solakyildirim K, Amster IJ, Linhardt RJ. Glycosaminoglycan characterization by electrospray ionization mass spectrometry including fourier transform mass spectrometry. Methods Enzymol. 2010;478:79–108.
- 66. Wong AW, Wang H, Lebrilla CB. Selection of Anionic Dopant for Quantifying Desialylation Reactions with MALDI-FTMS. Anal Chem. 2000;72(7):1419–25.
- 67. Zaia J. Principles of mass spectrometry of glycosaminoglycans. J Biomacromol Mass Spectrom. 2005;1(1):3–36.
- 68. Tóth G, Vékey K, Sugár S, Kovalszky I, Drahos L, Turiák L. Salt gradient chromatographic separation of chondroitin sulfate disaccharides. J Chromatogr A. 2020;1619:460979.
- 69. Tóth G, Vékey K, Drahos L, Horváth V, Turiák L. Salt and solvent effects in the

- microscale chromatographic separation of heparan sulfate disaccharides. J Chromatogr A. 2020, 1610: 460548.
- 70. Turiák L, Shao C, Meng L, Khatri K, Leymarie N, Wang Q, et al. Workflow for Combined Proteomics and Glycomics Profiling from Histological Tissues. Anal Chem. 2014;86(19):9670–8.
- 71. Hu H, Mao Y, Huang Y, Lin C, Zaia J. Bioinformatics of glycosaminoglycans. Perspect Sci. 2017;11:40–4.
- 72. Tóth G, Turiák L. HPLC-MS Characterization of Tissue-Derived Heparan Sulfate and Chondroitin Sulfate BT Proteoglycans: Methods and Protocols. In: Karamanos NK, editor. New York, NY: Springer US; 2023. p. 71–90.
- 73. Tóth G, Pál D, Vékey K, Drahos L, Turiák L. Stability and recovery issues concerning chondroitin sulfate disaccharide analysis. Anal Bioanal Chem. 2021;413(7): 1779-1785.
- 74. Volpi N, Mucci A, Schenetti L. Stability studies of chondroitin sulfate. Carbohydr Res. 1999;315(3):345–9.
- 75. Kozlowski AM, Yates EA, Roubroeks JP, Tømmeraas K, Smith AM, Morris GA. Hydrolytic Degradation of Heparin in Acidic Environments: Nuclear Magnetic Resonance Reveals Details of Selective Desulfation. ACS Appl Mater Interfaces. 2021;13(4):5551–63.
- 76. Anger P, Martinez C, Mourier P, Viskov C. Oligosaccharide Chromatographic Techniques for Quantitation of Structural Process-Related Impurities in Heparin Resulting From 2-O Desulfation [Internet]. Vol. 5, Frontiers in Medicine. 2018; 5: 346.
- 77. Jandik KA, Kruep D, Cartier M, Linhardt RJ. Accelerated stability studies of heparin. J Pharm Sci. 1996;85(1):45–51.
- 78. W.H. Organization. Global cancer burden growing, amidst mounting need for services. 2024.
- 79. Sung H, Ferlay J, Siegel RL, Laversanne M, Soerjomataram I, Jemal A, et al.

- Global Cancer Statistics 2020: GLOBOCAN Estimates of Incidence and Mortality Worldwide for 36 Cancers in 185 Countries. CA Cancer J Clin. 2021;71(3):209–49.
- 80. Nooreldeen R, Bach H. Current and Future Development in Lung Cancer Diagnosis. Vol. 22, Int. J. Mol. Sci. 2021; 22(16): 8661.
- 81. Inamura K. Lung Cancer: Understanding Its Molecular Pathology and the 2015 WHO Classification. Vol. 7, Frontiers in Oncology. 2017; 7: 193.
- 82. Ettinger DS, Akerley W, Bepler G, Blum MG, Chang A, Cheney RT, et al. Non-small cell lung cancer. J Natl Compr cancer Netw. 2010;8(7):740–801.
- 83. Travis WD. Pathology of lung cancer. Clin Chest Med. 2002;23(1):65–81.
- 84. Travis WD, Brambilla E, Riely GJ. New Pathologic Classification of Lung Cancer: Relevance for Clinical Practice and Clinical Trials. J Clin Oncol. 2013;31(8):992–1001.
- 85. Asada M, Furukawa K, Segawa K, Endo T, Kobata A. Increased Expression of Highly Branched N-Glycans at Cell Surface Is Correlated with the Malignant Phenotypes of Mouse Tumor Cells1. Cancer Res. 1997;57(6):1073–80.
- 86. Mi W, Gu Y, Han C, Liu H, Fan Q, Zhang X, et al. O-GlcNAcylation is a novel regulator of lung and colon cancer malignancy. Biochim Biophys Acta Mol Basis Dis. 2011;1812(4):514–9.
- 87. Kovalszky I, Pogany G, Molnar G, Jeney A, Lapis K, Karacsonyi S, et al. Altered glycosaminoglycan composition in reactive and neoplastic human liver. Biochem Biophys Res Commun. 1990;167(3):883–90.
- 88. Tóth G, Sugár S, Pál D, Fügedi KD, Drahos L, Schlosser G, et al. Glycosaminoglycan Analysis of FFPE Tissues from Prostate Cancer and Benign Prostate Hyperplasia Patients Reveals Altered Regulatory Functions and Independent Markers for Survival. Vol. 14, Cancers. 2022; 14(19): 4867.
- 89. Tóth G, Pál D, Sugár S, Kovalszky I, Dezső K, Schlosser G, et al. Expression of glycosaminoglycans in cirrhotic liver and hepatocellular carcinoma—a pilot study

- including etiology. Anal Bioanal Chem. 2022;414(13):3837–46.
- 90. Yoshiro Hatae , Tomoyoshi Atsuta AM. Glycosaminoglycans in human lung carcinoma. GANN Japanese J Cancer Res. 1977;68(1):59–63.
- 91. Horai T, Nakamura N, Tateishi R, Hattori S. Glycosaminoglycans in human lung cancer. Cancer. 1981;48(9):2016–21.
- 92. Li G, Li L, Joo EJ, Son JW, Kim YJ, Kang JK, et al. Glycosaminoglycans and glycolipids as potential biomarkers in lung cancer. Glycoconj J. 2017;34(5):661–9.
- 93. Kumar A, Kumar A. Non-small-cell lung cancer-associated gene mutations and inhibitors. Adv Cancer Biol Metastasis. 2022;6:100076.8
- 94. Passaro A, Attili I, Rappa A, Vacirca D, Ranghiero A, Fumagalli C, et al. Genomic Characterization of Concurrent Alterations in Non-Small Cell Lung Cancer (NSCLC) Harboring Actionable Mutations. Vol. 13, Cancers. 2021; 13(9): 2172.
- 95. Warth A, Penzel R, Lindenmaier H, Brandt R, Stenzinger A, Herpel E, et al. EGFR, KRAS, BRAF and ALK gene alterations in lung adenocarcinomas: patient outcome, interplay with morphology and immunophenotype. Eur Respir J. 2013;43(3):872–83.
- 96. Pikor LA, Ramnarine VR, Lam S, Lam WL. Genetic alterations defining NSCLC subtypes and their therapeutic implications. Lung Cancer. 2013;82(2):179–89.
- 97. Xiao Y, Liu P, Wei J, Zhang X, Guo J, Lin Y. Recent progress in targeted therapy for non-small cell lung cancer. Front Pharmacol. 2023; 14: 1125547.
- 98. Colombino M, Paliogiannis P, Cossu A, Santeufemia DA, Pazzola A, Fadda GM, et al. EGFR, KRAS, BRAF, ALK, and cMET genetic alterations in 1440 Sardinian patients with lung adenocarcinoma. BMC Pulm Med. 2019;19(1):209.
- 99. Lee B, Lee T, Lee S-H, Choi Y-L, Han J. Clinicopathologic characteristics of EGFR, KRAS, and ALK alterations in 6,595 lung cancers. Oncotarget. 2016;7(17):23874.
- 100. Li P, Gao Q, Jiang X, Zhan Z, Yan Q, Li Z, et al. Comparison of

- clinicopathological features and prognosis between ALK rearrangements and EGFR mutations in surgically resected early-stage lung adenocarcinoma. J Cancer. 2019;10(1):61.
- 101. Sharma S V, Bell DW, Settleman J, Haber DA. Epidermal growth factor receptor mutations in lung cancer. Nat Rev Cancer. 2007;7(3):169–81.
- 102. Russano M, Perrone G, Di Fazio GR, Galletti A, Citarella F, Santo V, et al. Uncommon EGFR mutations in non-small-cell lung cancer. Precis Cancer Med Vol 5,. 2022;5:30-30.
- 103. Devarakonda S, Morgensztern D, Govindan R. Genomic alterations in lung adenocarcinoma. Lancet Oncol. 2015;16(7):e342–51.
- 104. Ito M, Miyata Y, Kushitani K, Ueda D, Takeshima Y, Okada M. Distribution and prognostic impact of EGFR and KRAS mutations according to histological subtype and tumor invasion status in pTis-3N0M0 lung adenocarcinoma. BMC Cancer. 2023;23(1):248.
- 105. Cekani E, Epistolio S, Dazio G, Cefalì M, Wannesson L, Frattini M, et al. Molecular Biology and Therapeutic Perspectives for K-Ras Mutant Non-Small Cell Lung Cancers. Vol. 14, Cancers. 2022; 14(17): 4103.
- 106. Barreca A, Lasorsa E, Riera L, Machiorlatti R, Piva R, Ponzoni M, et al. Anaplastic lymphoma kinase in human cancer. J Mol Endocrinol. 2011;47(1):R11–23.
- 107. Samatar AA, Poulikakos PI. Targeting RAS–ERK signalling in cancer: promises and challenges. Nat Rev Drug Discov. 2014;13(12):928–42.
- 108. Fruman DA, Chiu H, Hopkins BD, Bagrodia S, Cantley LC, Abraham RT. The PI3K Pathway in Human Disease. Cell. 2017;170(4):605–35.
- 109. S. MT, Yi-Long W, Myung-Ju A, C. GM, R. KH, S. RS, et al. Osimertinib or Platinum-Pemetrexed in EGFR T790M-Positive Lung Cancer. N Engl J Med. 2025;376(7):629-40.
- 110. Pál D, Tóth G, Turiák L. Investigation of sample handling steps for accurate heparan sulphate disaccharide analysis using HPLC–MS. Electrophoresis. 2024.

- 111. Pál D, Tóth G, Sugár S, Fügedi KD, Szabó D, Kovalszky I, et al. Compositional Analysis of Glycosaminoglycans in Different Lung Cancer Types— A Pilot Study. Vol. 24, International Journal of Molecular Sciences. 2023;24(8): 7050.
- 112. Pál D, Bugyi F, Virág D, Szabó D, Schlosser G, Kovalszky I, et al. Analysis and characterization of chondroitin/dermatan sulfate composition of lung adenocarcinoma tissues with different types of genetic alterations in ALK, EGFR and KRAS oncogenes. Carbohydr Polym Technol Appl. 2025;10:100826.
- 113. Watanabe Y, Aoki-Kinoshita KF, Ishihama Y, Okuda S. GlycoPOST realizes FAIR principles for glycomics mass spectrometry data. Nucleic Acids Res. 2021;49(D1):D1523-8.
- 114. Zaia J, McClellan JE, Costello CE. Tandem Mass Spectrometric Determination of the 4S/6S Sulfation Sequence in Chondroitin Sulfate Oligosaccharides. Anal Chem. 2001;73(24):6030–9.
- 115. Desaire H, Leary JA. Detection and quantification of the sulfated disaccharides in chondroitin sulfate by electrospray tandem mass spectrometry. J Am Soc Mass Spectrom. 2000;11(10):916–20.
- 116. Eriksson C-G, Nordström L, Eneroth P. Formation of imine derivatives between Tris(hydroxymethyl)-aminomethane and saturated 3-oxo steroids during conventional work up of biological samples dissolved in Tris-HCl buffers. J Steroid Biochem. 1983;19(2):1199–203.
- 117. Mikami Y, Murata M. Effects of Sugar and Buffer Types, and pH on Formation of Maillard Pigments in the Lysine Model System. Food Sci Technol Res. 2015;21(6):813–9.
- 118. Huang Y, Mao Y, Zong C, Lin C, Boons G-J, Zaia J. Discovery of a Heparan Sulfate 3-O-Sulfation Specific Peeling Reaction. Anal Chem. 2015;87(1):592–600.
- 119. Shinmei M, Miyauchi S, Machida A, Miyazaki K. Quantitation of chondroitin 4-sulfate and chondroitin 6-sulfate in pathologic joint fluid. Arthritis Rheum. 1992;35(11):1304–8.

- 120. Yutsudo N, Kitagawa H. Involvement of chondroitin 6-sulfation in temporal lobe epilepsy. Exp Neurol. 2015;274(Pt B):126–33.
- 121. Blake MR, Parrish DC, Staffenson MA, Sueda S, Woodward WR, Habecker BA. Chondroitin sulfate proteoglycan 4,6 sulfation regulates sympathetic nerve regeneration after myocardial infarction. Shivkumar K, Zaidi M, Shivkumar K, Wang H, Rajendran PS, editors. Elife. 2022;11:e78387.
- 122. Reine TM, Grøndahl F, Jenssen TG, Hadler-Olsen E, Prydz K, Kolset SO. Reduced Sulfation of Chondroitin Sulfate but Not Heparan Sulfate in Kidneys of Diabetic db/db Mice. J Histochem Cytochem. 2013;61(8):606–16.
- 123. Biskup K, Stellmach C, Braicu EI, Sehouli J, Blanchard V. Chondroitin Sulfate Disaccharides, a Serum Marker for Primary Serous Epithelial Ovarian Cancer. Diagnostics (Basel, Switzerland). 2021;11(7).
- 124. Stephenson EL, Mishra MK, Moussienko D, Laflamme N, Rivest S, Ling C-C, et al. Chondroitin sulfate proteoglycans as novel drivers of leucocyte infiltration in multiple sclerosis. Brain. 2018;141(4):1094–110.
- 125. Cooney CA, Jousheghany F, Yao-Borengasser A, Phanavanh B, Gomes T, Kieber-Emmons AM, et al. Chondroitin sulfates play a major role in breast cancer metastasis: a role for CSPG4 and CHST11gene expression in forming surface P-selectin ligands in aggressive breast cancer cells. Breast Cancer Res. 2011;13(3):R58.
- 126. Kitazawa K, Nadanaka S, Kadomatsu K, Kitagawa H. Chondroitin 6-sulfate represses keratinocyte proliferation in mouse skin, which is associated with psoriasis. Commun Biol. 2021;4(1):114.
- 127. Oo HZ, Lohinai Z, Khazamipour N, Lo J, Kumar G, Pihl J, et al. Oncofetal Chondroitin Sulfate Is a Highly Expressed Therapeutic Target in Non-Small Cell Lung Cancer. Vol. 13, Cancers. 2021;13(17): 4489.
- 128. Spliid CB, Toledo AG, Sanderson P, Mao Y, Gatto F, Gustavsson T, et al. The specificity of the malarial VAR2CSA protein for chondroitin sulfate depends on 4-O-sulfation and ligand accessibility. J Biol Chem. 2021;297(6).

- 129. Kawai T, Suzuki M, Kageyama K. Glycosaminoglycans in lung carcinoma. Hum Pathol. 1988;19(11):1288–92.
- 130. Sugár S, Bugyi F, Tóth G, Pápay J, Kovalszky I, Tornóczky T, et al. Proteomic Analysis of Lung Cancer Types— A Pilot Study. Vol. 14, Cancers. 2022; 14(11): 2629.
- 131. Iozzo R V, Schaefer L. Proteoglycan form and function: A comprehensive nomenclature of proteoglycans. Matrix Biol. 2015;42:11–55.
- 132. Wight TN. Versican: a versatile extracellular matrix proteoglycan in cell biology. Curr Opin Cell Biol. 2002;14(5):617–23.
- 133. Nastase Madalina V, Young Marian F, Schaefer Liliana. Biglycan: A Multivalent Proteoglycan Providing Structure and Signals. J Histochem Cytochem. 2012;60(12):963–75.
- 134. Toledo AG, Pihl J, Spliid CB, Persson A, Nilsson J, Pereira MA, et al. An affinity chromatography and glycoproteomics workflow to profile the chondroitin sulfate proteoglycans that interact with malarial VAR2CSA in the placenta and in cancer. Glycobiology. 2020;30(12):989–1002.
- 135. Guo J-Y, Chiu C-H, Wang M-J, Li F-A, Chen J-Y. Proteoglycan serglycin promotes non-small cell lung cancer cell migration through the interaction of its glycosaminoglycans with CD44. J Biomed Sci. 2020;27(1):2.
- 136. Pudełko A, Wisowski G, Olczyk K, Koźma EM. The dual role of the glycosaminoglycan chondroitin-6-sulfate in the development, progression and metastasis of cancer. FEBS J. 2019;286(10):1815–37.
- 137. Lanzi C, Cassinelli G. Receptor tyrosine kinases and heparan sulfate proteoglycans: Interplay providing anticancer targeting strategies and new therapeutic opportunities. Biochem Pharmacol. 2020;178:114084.
- 138. Bugyi F, Balbisi M, Sugár S, Váncza L, Regős E, Kovalszky I, et al. Unveiling unique protein and phosphorylation signatures in lung adenocarcinomas with and without ALK, EGFR, and KRAS genetic alterations. Mol Oncol. 2025.

- 139. Morimoto H, Hida Y, Maishi N, Nishihara H, Hatanaka Y, Li C, et al. Biglycan, tumor endothelial cell secreting proteoglycan, as possible biomarker for lung cancer. Thorac cancer. 2021;12(9):1347–57.
- 140. Clausen TM, Pereira MA, Al Nakouzi N, Oo HZ, Agerbæk MØ, Lee S, et al. Oncofetal Chondroitin Sulfate Glycosaminoglycans Are Key Players in Integrin Signaling and Tumor Cell Motility. Mol Cancer Res. 2016;14(12):1288–99.
- 141. Salanti A, Clausen TM, Agerbæk MØ, Al Nakouzi N, Dahlbäck M, Oo HZ, et al. Targeting Human Cancer by a Glycosaminoglycan Binding Malaria Protein. Cancer Cell. 2015;28(4):500–14.
- 142. Seiler R, Oo HZ, Tortora D, Clausen TM, Wang CK, Kumar G, et al. An Oncofetal Glycosaminoglycan Modification Provides Therapeutic Access to Cisplatin-resistant Bladder Cancer. Eur Urol. 2017;72(1):142–50.
- 143. Machino M, Gong Y, Ozaki T, Suzuki Y, Watanabe E, Imagama S, et al. Dermatan sulphate is an activating ligand of anaplastic lymphoma kinase. J Biochem. 2021;170(5):631–7.
- 144. Popat S, Hsia T-C, Hung J-Y, Jung HA, Shih J-Y, Park CK, et al. Tyrosine Kinase Inhibitor Activity in Patients with NSCLC Harboring Uncommon EGFR Mutations: A Retrospective International Cohort Study (UpSwinG). Oncologist. 2022;27(4):255–65.
- 145. Murray PB, Lax I, Reshetnyak A, Ligon GF, Lillquist JS, Natoli EJ, et al. Heparin is an activating ligand of the orphan receptor tyrosine kinase ALK. Sci Signal. 2015;8(360):ra6–ra6.

9. Bibliography of the candidate's publications

9.1. Publications Related to the Dissertation

1.

<u>Pál, D.</u>, Tóth, G., Turiák, L. Investigation of sample handling steps for accurate heparan sulfate disaccharide analysis using HPLC–MS. *Electrophoresis* 2024, 1–14. https://doi.org/10.1002/elps.202400091

IF: 3.0; Q2

2.

<u>Pál, D.</u>, Tóth, G., Sugár, S., Fügedi, K.D., Szabó, D., Kovalszky, I., Papp, D., Schlosser, G., Tóth, C., Tornóczky, T., Drahos, L., Turiák, L. Compositional analysis of glycosaminoglycans in different lung cancer types—a pilot study. *International Journal of Molecular Sciences* 2023, 24, 7050.

https://doi.org/10.3390/ijms24087050

IF: 4.9; D1

3.

<u>Pál, D.</u>, Fanni, B., Virág, D., Szabó, D., Schlosser, G., Kovalszky, I., Harkó, T., Moldvay, J., Turiák, L. Analysis and charachterization of chondroitin/dermatan sulfate composition of lung adenocarcinoma tissues with different types of genetic alterations in ALK, EGFR and KRAS oncogenes. *Carbohydrate Polymer Technologies and Applications* 2025, 100826.

https://doi.org/10.1016/j.carpta.2025.100826

IF: 6.2; Q1

9.2. Publications Unrelated to the Dissertation

4.

Tóth, G., <u>Pál, D.</u>, Vékey, K., Drahos, L., Turiák, *L.* Stability and recovery issues concerning chondroitin sulfate disaccharide analysis. *Analytical and Bioanalytical Chemistry* 2021, 413, 1779–1785.

https://doi.org/10.1007/s00216-021-03152-7

IF: 4.478; Q1

5.

Tóth, G., <u>Pál, D.</u>, Sugár, S. Kovalszky, I., Dezső, K., Schlosser, G., Drahos, L., Turiák, L. Expression of glycosaminoglycans in cirrhotic liver and hepatocellular carcinoma—a pilot study including etiology. *Analytical and Bioanalytical Chemistry* 2022, 414, 3837–3846.

https://doi.org/10.1007/s00216-022-04025-3

IF: 4.3; Q2

6.

Tóth, G., Sugár, S., <u>Pál, D.</u>, Fügedi, K.D., Drahos, L., Schlosser, G., Oláh, C., Reis, H., Kovalszky, I., Szarvas, T., Turiák, L. Glycosaminoglycan analysis of FFPE tissues from prostate cancer and benign prostate hyperplasia patients reveals altered regulatory functions and independent markers for survival. *Cancers* 2022,14, 4867. https://doi.org/10.3390/cancers14194867

IF: 5.2; Q1

7.

Balbisi, M., Langó, T., Horváth, V.N., <u>Pál, D.</u>, Schlosser, G., Kecskeméti, G., Szabó, Z., Ilyés, K., Nagy, N., Tóth, O., Visnovitz, T., Varga, Z., Vértessy, B.G., Turiák, L. A549 tumorigenic and BEAS-2B non-tumorigenic cell line-derived small extracellular vesicles show distinct proteomic, *N*-glycoproteomic, and chondroitin/dermatan sulfate profiles. *bioRxiv* 2025, 03.13.643059.

https://doi.org/10.1101/2025.03.13.643059 (PREPRINT)

10. Acknowledgements

I would like to express my sincere gratitude to my supervisor, Lilla Turiák, for her invaluable work, her continuous support and encouragement throughout my MSc work until the completion of my PhD studies. Her expertise and mentorship were indispensable in the preparation of this dissertation. Especially I would also like to thank my former cosupervisor Gábor Tóth, who gave me a deeper insight into the world of mass spectrometry and the analytical investigation of glycosaminoglycans.

I would like to thank Dávid Virág for his outstanding helpfulness during my research and PhD work. Special thanks to Ágnes Gömöry, who has always been helpful with her professional knowledge in the field of mass spectrometry.

I am grateful to Gitta Schlosser for providing us the analytical instrument of the MTA-ELTE Lendület Ion Mobility Mass Spectrometry Research Group for our investigations. I would like to thank Judit Moldvay for providing us the samples that were essential for our research.

I am grateful to all the former and present members of the MS Proteomics Research Group and MTA-HUN-REN TTK Lendület (Momentum) Glycan Biomarker Research Group who have contributed in any way to my work: László Drahos, Károly Vékey, András Ács, Simon Sugár, Ágnes Révész, Fanni Bugyi, Dániel Szabó, Balázs Molnár, Kata Fügedi, Kinga Nagy, Mirjam Balbisi, Virág Horváth, Rachma Dessidianti Nur Hidayat, Alexandra Molnár, Boglárka Cziráki, Krisztián Karvaly.

I am grateful to my parents and grandparents for their outstanding support and motivation. I would also like to thank my loved ones for their constant encouragement, patience, and understanding, which have been invaluable throughout this journey.

I would like to thank the Doctoral School of Semmelweis University, Pharmaceutical Sciences and Health Technologies Division and institutes of HUN-REN Research Centre for Natural Sciences.